Journal of Scientific Computing (2025) 105:2
https://doi.org/10.1007/s10915-025-03025-6

Numerical Approximation of a Nonlinear Age-Structured Population Model with Finite Life-Span

Luis M. Abia[1] · **Óscar Angulo**[1] · **Juan Carlos López-Marcos**[1] · **Miguel Ángel López-Marcos**[1]

Received: 28 March 2025 / Revised: 26 July 2025 / Accepted: 5 August 2025 /
Published online: 19 August 2025

Abstract
We introduce a numerical method which is developed to approach the solution to a nonlinear age-structured population model with a finite life-span. The new scheme employs given numerical approximations to the intrinsic survival probability to set a full discretization of the problem, in which the numerical approach to the age-specific density of the population is separated from the difficulties arising due to the singular mortality rate. Its convergence is completely established without an explicit dependence on the asymptotic behaviour of the natural mortality rate near the maximum age. We include a numerical experimentation that confirms numerically the second-order convergence of the approximations provided by the corresponding theorems.

Keywords Nonlinear problem · Age-structured population · Finite life-span · Survival probability · Numerical methods · Characteristics method · Convergence analysis

Mathematics Subject Classification MSC 92D25 · MSC 65M25 · 65M12

1 Introduction

We consider an age-structured population model with a finite life-span

$$u_t + u_a = -\mu(a, I_\mu(t), t)\, u, \quad 0 < a < a_\dagger, \ t > 0, \tag{1}$$

$$u(0, t) = \int_0^{a_\dagger} \beta(a, I_\beta(t), t)\, u(a, t)\, da\ , \quad t > 0, \tag{2}$$

✉ Miguel Ángel López-Marcos
malm@uva.es

Luis M. Abia
lmabia@uva.es

Óscar Angulo
oscar.angulo@uva.es

Juan Carlos López-Marcos
lopezmar@uva.es

[1] Departamento de Matemática Aplicada & IMUVa, Facultad de Ciencias, Universidad de Valladolid, Paseo de Belén 7 - Campus Miguel Delibes, 47011 Valladolid, Spain

$$u(a, 0) = u^0(a), \quad 0 \le a < a_\dagger. \tag{3}$$

Here, the argument $a \in [0, a_\dagger]$ represents age, where $a_\dagger$ denotes the maximum age of individuals in the population, $t \ge 0$ represents time and $u(a, t)$ gives the density function for the age-distribution of the individuals in the population at time t.

Equation (1) describes the balance of individuals in the population through the aging and death processes. We consider a nonnegative mortality rate function $\mu(a, I_\mu(t), t)$ that is given in a separable form as

$$\mu(a, I_\mu(t), t) = \mu_0(a) + \mu_b(a, I_\mu(t), t), \tag{4}$$

to discern between the natural mortality rate, μ_0, depending only on age, and a bounded mortality rate term, μ_b. The natural mortality rate, $\mu_0(a)$, is nonnegative and satisfies the following hypothesis

$$\int_0^{a_\dagger} \mu_0(s) ds = +\infty. \tag{5}$$

The function μ_b gives an account of the variability of the mortality rate due to seasonal factors and the competition among individuals, as represented by the dependence on the functional

$$I_\mu(t) = \int_0^{a_\dagger} \gamma_\mu(a)\, u(a, t)\, da, \quad t \ge 0, \tag{6}$$

with $\gamma_\mu(a) \ge 0$, $a \in [0, a_\dagger]$. We also assume $\mu_b(a, 0, t) = 0$, a.e. $a \in [0, a_\dagger]$.

For convenience, we introduce the survival functions [11]

$$\pi_0(a) = \exp\left(-\int_0^a \mu_0(s)\, ds\right), \quad 0 \le a < a_\dagger, \tag{7}$$

and

$$\pi(a, t) = \pi_0(a) \exp\left(-\int_0^a \mu_b(s, I_\mu(t - a + s), t - a + s)\, ds\right), \ 0 \le a < a_\dagger,\ t \ge a, \tag{8}$$

that gives the probability that an individual that was born at time $t - a$ will survive up to time t with age a. We call $\pi_0(a)$ as the intrinsic survival probability, and should decrease to zero as the age increases to $a_\dagger$ because the assumption (5). Negative values of μ_b are not excluded, they only mean that the probability of an individual to survive given by (8) might be greater than the intrinsic survival probability (7), due to external factors.

The birth-law for individuals is given by the condition (2) with a nonnegative fertility rate function $\beta(a, I_\beta(t), t)$ that also depends on a functional

$$I_\beta(t) = \int_0^{a_\dagger} \gamma_\beta(a)\, u(a, t)\, da\ , \quad t \ge 0, \tag{9}$$

with $\gamma_\beta(a) \ge 0$, $a \in [0, a_\dagger]$, to represent again the competition. By restricting the support of function $\gamma_\beta(a)$ to an appropriate compact subinterval of $[0, a_\dagger]$, we also model the age-fertility windows for individuals in the population. Finally, the nonnegative function u^0 in (3) describes the initial age-distribution of the individuals in the population.

On the one hand, a finite life-span age-structured population model with maximum age $a_\dagger < \infty$ appears biologically more realistic than models with infinite life-span. In those models, the mortality rate function must blow-up close to $a_\dagger$ to force that individuals die before the maximum age (existence, uniqueness and regularity of solutions of these models in appropriate function spaces were already considered in the monographs [11, 12]). On the other hand, it is usual to associate the unbounded behaviour of the mortality nearby the maximum age to a natural age-dependent mortality term, μ_0 (note assumption (5)), and to isolate it from seasonal and density dependent effects on the mortality rate that can be introduced in a bounded mortality term, μ_b, as in (4).

The difficulties produced in the numerical treatment of the singularity in the natural age-dependent mortality rate were investigated in [1, 13] by assuming a specific behaviour for the growth of the mortality in a neighbourhood of the maximum age, $[a_*, a_\dagger)$, which is generally stated in the form of a negative power-law bound

$$\mu_0(a) \leq \frac{\lambda}{(a_\dagger - a)^\alpha}, \quad a \in [a_*, a_\dagger), \quad \alpha \geq 1, \quad \lambda > 0, \tag{10}$$

with $0 \leq a_* < a_\dagger$ and $\mu_0(a_*) = \max_{a\in[0,a_*]} \mu_0(a)$. It is shown that the order of convergence of the numerical approximations considered for the intrinsic survival probability (7) is strongly dependent on the parameters $\alpha \geq 1$, $\lambda > 0$, that model the asymptotic behaviour of the natural mortality, μ_0.

Consequently, the numerical solution of (1)-(3) is also affected by the unbounded nature of the mortality. To circumvent the obstacles, some authors require a detailed knowledge of this rate [1–10, 14–17, 19, 20]. In particular, for the linear problem with $\mu_b = 0$ and $\beta = \beta(a)$, in [2] we propose a method for the numerical solution of the problem using second-order approximations for the intrinsic survival probability, irrespective of the particular technique by which these estimates have been obtained. Thus, in that case, it is not necessary to assume a specific behaviour in the asymptotic growth of μ_0 as, for example, in (10). A straightforward analysis of the propagation of the quadrature errors in the discretization allows us to ensure that the error committed by the numerical solution when approximating the grid restriction of the exact solution goes to zero as the discretisation parameter decreases. More precisely, it is established that the method provides second-order approximations assuming certain acceptable regularity conditions on the unknown exact solution.

In this paper, we extend the previous approach to the nonlinear problem (1)-(3): we decouple the task of obtaining estimates to the intrinsic survival probability from that of calculating approximations to the solution of the problem. Again, having second-order approximations to the survival function in advance will allow us to design a discretization technique that provides numerical estimates to the population density function, with the same second-order of convergence. In this case, we prove the second-order of convergence using a different technique than the one used in [2] for the linear case: now it is based on the analysis of consistence and nonlinear stability properties of the discretization.

In Section 2, we introduce the numerical procedure which is developed to approximate the solution to problem (1)-(3). Section 3 is devoted to the complete analysis of the convergence of this numerical method. Section 4 shows the numerical experimentation that confirms numerically the theoretical results. Section 5 concludes.

2 Numerical approximation

In addition to the non-linearity of the model, the singularity of the natural mortality rate μ_0, at the maximum age $a_\dagger$, is the main challenge to develop the numerical approximation of problem (1)-(3). Our approach to the model considers a change of variable with the relationship, assuming that $\pi_0 \in \mathcal{C}^1([0, a_\dagger))$,

$$u(a,t) = \pi_0(a)\, v(a,t), \quad 0 \leq a < a_\dagger, \tag{11}$$

and reformulates the boundary and initial value problem (1)-(3) in terms of the new dependent variable $v(a, t)$. Therefore, taking into account that $\pi_0'(a) = -\mu_0(a)\pi_0(a)$, and dividing by $\pi_0(a) \neq 0$, function v satisfies

$$v_t + v_a = -\mu_b(a, I_\mu(t), t)\, v, \quad 0 < a < a_\dagger,\ t > 0, \tag{12}$$

$$v(0, t) = \int_0^{a_\dagger} \pi_0(a)\, \beta(a, I_\beta(t), t)\, v(a, t)\, da\ , \quad t > 0, \tag{13}$$

$$v(a, 0) = \frac{u^0(a)}{\pi_0(a)}, \quad 0 \le a < a_\dagger, \tag{14}$$

with nonlocal terms

$$I_\mu(t) = \int_0^{a_\dagger} \pi_0(a)\gamma_\mu(a)v(a, t)\, da, \quad I_\beta(t) = \int_0^{a_\dagger} \pi_0(a)\gamma_\beta(a)v(a, t)\, da\ ,\ t \ge 0. \tag{15}$$

Besides, in order to ensure that the function v is bounded over $[0, a_\dagger)$ at the initial time, we impose that

$$\lim_{a \to a_\dagger} \frac{u^0(a)}{\pi_0(a)} < \infty. \tag{16}$$

We emphasize that the unbounded natural mortality rate μ_0 only appears in the new problem (12)-(14) through the intrinsic survival probability π_0: in the nonlocal functional terms $I_\mu(t)$ and $I_\beta(t)$ defined by (15), and which are involved in (12) and (13), respectively; in the birth law (13); and in the new initial condition (14). Therefore, the new balance law (12) does not longer include any singular term and, on the other hand, the new non-local terms only incorporate the survival probability π_0, which is already a bounded function and does not introduce any singularity. In conclusion, assuming (16), by discretizing problem (12)-(14), we circumvent the difficulties coming from the singularity of the natural mortality rate when analysing the convergence of the approximations to the solution v.

First, we discretize the age variable. For convenience, we suppose that there exists a value for age a_*, $0 < a_* < a_\dagger$, that represents an important characteristic of the model to be taken into account. For example, from a theoretical point of view, when a_* fixes an appropriate asymptotic growth behaviour as in (10). Also, from an experimental point of view, when modeling the intrinsic survival probability π_0, from census data: using a piecewise polynomial function representation in the subinterval $[0, a_*]$, and an appropriate least-squares approximation using a model function for the growth of the mortality in the subinterval $[a_*, a_\dagger)$, can be useful.

Therefore, given a positive integer J^*, we define the step size (the discretization parameter) as $h = a_*/J^*$. Then, we introduce the discrete ages $a_j = j\, h$, $j = 0, 1, \ldots, J$, where J is the closest integer strictly less than $a_\dagger/h$. As a result, $a_{J^*} = a_*$ and $0 < a_\dagger - a_J \le h$.

In contrast, if there is no highlighted age like a_*, the discretization of the age variable is as follows: for a positive integer J, let us define $h = a_\dagger/(J+1)$ as the discretization parameter. Again $a_j = j\, h$, $j = 0, 1, \ldots, J$, and then $a_J = J\, h$, satisfies $0 < a_\dagger - a_J = h$.

Next, assuming that we are going to perform the numerical integration on a bounded time interval $[0, T]$, $T > 0$, we use the same step size h for the discretization of the time variable. Therefore, we introduce the discrete times $t^n = n\, h$, $n = 0, 1, \ldots, N$, where $N = \lfloor T/h \rfloor$. We use the following vector notation: at each time level t^n, $n = 0, 1, \ldots, N$, the numerical solution is described by a $(J+1)$-dimensional vector $\mathbf{V}^n = (V_0^n, V_1^n, \ldots, V_J^n)$, where V_j^n would be the numerical approximation to $v(a_j, t^n)$, $j = 0, 1, \ldots, J$, solution of (12)-(14). Vector $\boldsymbol{\Pi} = (\Pi_0, \Pi_1, \ldots, \Pi_J)$, with capital letters, recovers the approximations to the intrinsic survival vector $\boldsymbol{\pi}_0 = (\pi_0(a_0), \pi_0(a_1), \ldots, \pi_0(a_J))$, in lower case. That is, Π_j is an approximation to $\pi_0(a_j)$, $j = 0, 1 \ldots, J$, which is obtained by approximation of π_0 in (7) with a numerical method, or from an appropriate modelling of this survival function.

We assume, from now on, that $\boldsymbol{\Pi} = (\Pi_0, \Pi_1, \ldots, \Pi_J)$, contains positive second-order approximations to the intrinsic survival probability of the population:

(H0) $\Pi_j > 0$, $j = 0, 1, \ldots, J$, and $\max_{j=0,\ldots,J} |\Pi_j - \pi_0(a_j)| = \mathcal{O}(h^2)$, as $h \to 0$.

The condition $\Pi_j > 0$, $j = 0, 1, \ldots, J$, can be easily satisfied if these approximations to (7) are obtained by exponentials of a quadrature rule (as in [1]), or it can be imposed when modeling the intrinsic survival probability of the population from field data. In this way, we separate the problem of approaching the intrinsic survival probability π_0, from the approximation of the density function v.

First we rewrite the new balance law. Note that the solution of (12) satisfies, for each $t > 0$, $a \in (0, a_\dagger)$, and each $h > 0$, such that $a + h < a_\dagger$,

$$v(a+h, t+h) = v(a,t)\, \exp\left(-\int_0^h \mu_b\left(a+s, I_\mu(t+s), t+s\right) ds\right). \tag{17}$$

For practical reasons, to approximate the integrals that appear in the boundary condition (13), and in the arguments of functions β and μ_b (that is, the nonlocal terms described in (15)), we use the same open quadrature rule as in [2]: for a vector $\mathbf{Y} = (Y_0, Y_1, \ldots, Y_J)$, we define

$$\mathcal{Q}_h(\mathbf{Y}) = h\, Y_1 + \sum_{j=1}^{J-1} \frac{h}{2}\, \left(Y_{j+1} + Y_j\right)) + (a_\dagger - a_J)\, Y_J. \tag{18}$$

Thus, given a suitable approximation $\mathbf{V}^0$, to the initial condition (14), we perform the evolution in time of the numerical method computing $\mathbf{V}^{n+1}$, $n = 0, 1, \ldots, N-1$, from $\mathbf{V}^n$, the approximation to the solution at the previous time-step. To do so, we first calculate an auxiliary approximation, represented by $\mathbf{V}^{n+1,*} = (V_0^{n+1,*}, V_1^{n+1,*}, \ldots, V_J^{n+1,*})$, obtained from $\mathbf{V}^n$ and which is subsequently used to compute $\mathbf{V}^{n+1}$, $n = 0, 1, \ldots, N-1$.

The scheme, based on the discretization of (17) and (13), is described component-wise as follows: for $n = 0, 1, \ldots, N-1$, and $j = 0, 1, \ldots, J-1$

$$V_{j+1}^{n+1,*} = V_j^n \exp\left(-h\, \mu_b\left(a_j, \mathcal{Q}_h(\boldsymbol{\Pi} \cdot \boldsymbol{\gamma}_\mu \cdot \mathbf{V}^n), t^n\right)\right), \tag{19}$$

$$V_0^{n+1,*} = \mathcal{Q}_h(\boldsymbol{\Pi} \cdot \boldsymbol{\beta}^{n+1,*} \cdot \mathbf{V}^{n+1,*}), \tag{20}$$

$$\begin{aligned} V_{j+1}^{n+1} = V_j^n \exp\Bigg(-\frac{h}{2}\Big[&\mu_b\big(a_j, \mathcal{Q}_h(\boldsymbol{\Pi} \cdot \boldsymbol{\gamma}_\mu \cdot \mathbf{V}^n), t^n\big) \\ &+\mu_b\left(a_{j+1}, \mathcal{Q}_h(\boldsymbol{\Pi} \cdot \boldsymbol{\gamma}_\mu \cdot \mathbf{V}^{n+1,*}), t^{n+1}\right)\Big]\Bigg), \end{aligned} \tag{21}$$

$$V_0^{n+1} = \mathcal{Q}_h(\boldsymbol{\Pi} \cdot \boldsymbol{\beta}^{n+1} \cdot \mathbf{V}^{n+1}). \tag{22}$$

The components of vectors $\boldsymbol{\gamma}_\mu$, $\boldsymbol{\gamma}_\beta$, $\boldsymbol{\beta}^{n+1}$, and $\boldsymbol{\beta}^{n+1,*}$, $n = 0, 1, \ldots, N-1$, are described, for $j = 0, 1, \ldots, J$, as

$$\begin{aligned} (\gamma_\mu)_j &= \gamma_\mu(a_j), \qquad & \beta_j^{n+1} &= \beta(a_j, \mathcal{Q}_h(\boldsymbol{\Pi} \cdot \boldsymbol{\gamma}_\beta \cdot \mathbf{V}^{n+1}), t^{n+1}), \\ (\gamma_\beta)_j &= \gamma_\beta(a_j), & \beta_j^{n+1,*} &= \beta(a_j, \mathcal{Q}_h(\boldsymbol{\Pi} \cdot \boldsymbol{\gamma}_\beta \cdot \mathbf{V}^{n+1,*}), t^{n+1}). \end{aligned}$$

Finally, the products $\boldsymbol{\Pi} \cdot \boldsymbol{\gamma}_{\mu} \cdot \mathbf{V}^{n}$; $\boldsymbol{\Pi} \cdot \boldsymbol{\gamma}_{\mu} \cdot \mathbf{V}^{n+1,*}$; $\boldsymbol{\Pi} \cdot \boldsymbol{\beta}^{n+1} \cdot \mathbf{V}^{n+1}$; $\boldsymbol{\Pi} \cdot \boldsymbol{\beta}^{n+1,*} \cdot \mathbf{V}^{n+1,*}$; $\boldsymbol{\Pi} \cdot \boldsymbol{\gamma}_{\beta} \cdot \mathbf{V}^{n+1}$ and $\boldsymbol{\Pi} \cdot \boldsymbol{\gamma}_{\beta} \cdot \mathbf{V}^{n+1,*}$, $n = 0, 1, \ldots, N-1$, represent the element-wise product of the corresponding vectors.

Remember that the quadrature rule (18) does not require the first component of the vector where it is applied. Then, in the effective implementation of the method, it is unnecessary to calculate $V_0^{n+1,*}$, $n = 0, 1, \ldots, N-1$, (the first component of $\mathbf{V}^{n+1,*}$ defined by (20)), because it is not requiered in order to compute $\mathcal{Q}_h(\boldsymbol{\Pi} \cdot \boldsymbol{\gamma}_{\mu} \cdot \mathbf{V}^{n+1,*})$ in (21), and therefore, for obtaining $\mathbf{V}^{n+1}$. However, if a quadrature rule that is not open on the left were used, it would be mandatory to compute (20).

Finally, we describe the process to obtain the numerical approximation of the solution to the original problem (1)-(3), by means of the numerical approach computed with the method previously presented, for the solution to the problem (12)-(14) which appears after the change of variable (11). Again, at each time level t^n, $n = 0, 1, \ldots, N$, the numerical solution is described by a (J+1)-dimensional vector $\mathbf{U}^n = (U_0^n, U_1^n, \ldots, U_J^n)$, where U_j^n represents the numerical approximation to $u(a_j, t^n)$, $j = 0, 1, \ldots, J$, the values of the solution to (1)-(3) on the established age-time meshgrid.

Therefore, the numerical procedure requieres the following steps:

- **Preprocessing**: Given a numerical approximation $\mathbf{U}^0$ to the initial condition (3), we define $\mathbf{V}^0$ with components, for $j = 0, 1, \ldots, J$,

$$V_j^0 = \frac{U_j^0}{\Pi_j}. \tag{23}$$

- **Time evolution**: We compute at each time level t^{n+1}, $n = 0, 1, \ldots N-1$, the approximation $\mathbf{V}^{n+1}$ of the solution to (12)-(14), by means of (19)-(22).
- **Postprocessing**: We obtain the approximation $\mathbf{U}^{n+1}$, $n = 0, 1, \ldots N-1$, of the solution to the original problem (1)-(3), with components, for $j = 0, 1, \ldots, J$,

$$U_j^{n+1} = \Pi_j \cdot V_j^{n+1}. \tag{24}$$

3 Convergence

In this section, we investigate the converge property of the procedure (23), (19)-(22), (24), introduced in Section 2, that approaches the solution to the problem (1)-(3).

To this end, previously we analyze the numerical method (19)-(22) for the approximation of the solution to (12)-(13). We emphasize that the values of the function $v(a, t)$ within the integrals (13) and (15), always appear as the product $\pi_0(a)\, v(a, t)$, that is, as the values of $u(a, t)$ due to (11). Therefore, in the following, the discretization errors for the numerical method (19)-(22) are analised assuming smoothness assumptions on the function $u(x, t)$, and some additional requirements on $v(a, t)$. Thus, let be $T > 0$ the final time, and let us suppose that

(H1) $u \in \mathcal{C}^2([0, a_\dagger] \times [0, T])$, $\pi_0 \in \mathcal{C}^2([0, a_\dagger))$, and $v(a, t) := u(a, t)/\pi_0(a)$ is bounded in $[0, a_\dagger) \times [0, T]$.

(H2) $\gamma_\mu, \gamma_\beta \in \mathcal{C}^2([0, a_\dagger])$, are nonnegative.

(H3) $\beta \in \mathcal{C}^2([0, a_\dagger] \times D_\beta \times [0, T])$, is nonnegative, where D_β is a compact neighbourghood of

$$\left\{I_\beta(t),\ 0 \le t \le T\right\} = \left\{\int_0^{a_\dagger} \pi_0(a)\,\gamma_\beta(a)\,v(a,t)\,da,\ 0 \le t \le T\right\}$$
$$= \left\{\int_0^{a_\dagger} \gamma_\beta(a)\,u(a,t)\,da,\ 0 \le t \le T\right\}.$$

(H4) $\mu_b \in \mathcal{C}^2([0, a_\dagger] \times D_\mu \times [0, T])$, where D_μ is a compact neighbourghood of

$$\left\{I_\mu(t),\ 0 \le t \le T\right\} = \left\{\int_0^{a_\dagger} \pi_0(a)\,\gamma_\mu(a)\,v(a,t)\,da,\ 0 \le t \le T\right\}$$
$$= \left\{\int_0^{a_\dagger} \gamma_\mu(a)\,u(a,t)\,da,\ 0 \le t \le T\right\}.$$

Notice that the second-order smoothness with respect to the age variable in the compact $[0, a_\dagger]$ (that appears in (H1) for the solution u, and in (H2)-(H4) for the data functions) is the minimum requirement to achieve second order of convergence for the numerical quadratures involved in obtaining the numerical approximation.

The convergence analysis will be addressed with the study of the consistency and nonlinear stability properties of the numerical scheme. We shall employ the discretization framework introduced by J.C. López-Marcos and J.M. Sanz-Serna (see [18]), then we describe the numerical integration adapted to it. Thus, we assume that the discretization parameter h takes values in the set $H = \{h > 0\,|\,h = a_*/J^*,\ J^* \in \mathbb{N}\}$, and for each $h \in H$, J is defined as the closest integer strictly lower than $a_\dagger/h$, and we consider the vector spaces $\mathcal{X}_h = (\mathbb{R}^{J+1})^{N+1}$ and $\mathcal{Y}_h = \mathbb{R}^{J+1} \times \mathbb{R}^N \times (\mathbb{R}^J)^N$. In the case where no significant age a_* has to be taken into account, we consider $H = \{h > 0\,|\,h = a_\dagger/(J+1),\ J \in \mathbb{N}\}$ to define $\mathcal{X}_h$ and $\mathcal{Y}_h$.

Now, we endow both spaces with suitable norms. Note that in the definition of $\mathcal{X}_h$ and $\mathcal{Y}_h$ appear Cartesian products of $\mathbb{R}^{L+1}$, $L = J-1, J, N-1$, so for $\mathbf{Y} = (Y_0, Y_1, \ldots, Y_L) \in \mathbb{R}^{L+1}$, we use the discrete $\mathcal{L}_\infty$ norm

$$\|\mathbf{Y}\|_{\infty,L+1} = \max_{j=0,\ldots,L} |Y_j|.$$

Taking into account that the quadrature rule (18) does not depend on Y_0, the first component of vector $\mathbf{Y} = (Y_0, Y_1, \ldots, Y_J) \in \mathbb{R}^{J+1}$, we also consider the seminorm

$$|\mathbf{Y}|_{\infty,J+1} = \max_{j=1,\ldots,J} |Y_j|,$$

where $|\mathbf{Y}|_{\infty,J+1} \le \|\mathbf{Y}\|_{\infty,J+1}$.

In the analysis, we also use the discrete $\mathcal{L}_1$ norm and seminorm in $\mathbb{R}^{J+1}$: for $\mathbf{Y} = (Y_0, Y_1, \ldots, Y_J)$

$$\|\mathbf{Y}\|_1 = \sum_{j=0}^{J} h\,|Y_j|, \qquad |\mathbf{Y}|_1 = \sum_{j=1}^{J} h\,|Y_j|,$$

respectively. Now $|\mathbf{Y}|_1 \le \|\mathbf{Y}\|_1$ and note that

$$\|\mathbf{Y}\|_1 \le (J+1)\,h\,\|\mathbf{Y}\|_{\infty,J+1} \le (a_\dagger + h)\,\|\mathbf{Y}\|_{\infty,J+1} \le 2\,a_\dagger\,\|\mathbf{Y}\|_{\infty,J+1}, \tag{25}$$

and, similarly

$$|\mathbf{Y}|_1 \le a_\dagger\,|\mathbf{Y}|_{\infty,J+1}. \tag{26}$$

Therefore, if $\mathbf{Y} = (Y_0, Y_1, \ldots, Y_J)$ and $\mathbf{Z} = (Z_0, Z_1, \ldots, Z_J)$ are in $\mathbb{R}^{J+1}$, and $\mathbf{Y} \cdot \mathbf{Z}$ represents the element-wise multiplication of the vectors, then

$$|\mathcal{Q}_h(\mathbf{Y} \cdot \mathbf{Z})| \leq \frac{3}{2} h |Y_1 Z_1| + \sum_{j=2}^{J-1} h |Y_j Z_j| + \frac{3}{2} h |Y_J Z_J| \leq \frac{3}{2} \|\mathbf{Y}\|_{\infty, J+1} |\mathbf{Z}|_1. \tag{27}$$

As a consequence, from (26)

$$|\mathcal{Q}_h(\mathbf{Y} \cdot \mathbf{Z})| \leq \frac{3}{2} a_\dagger \|\mathbf{Y}\|_{\infty, J+1} |\mathbf{Z}|_{\infty, J+1}, \tag{28}$$

and, in particular

$$|\mathcal{Q}_h(\mathbf{Y} \cdot \mathbf{Z})| \leq \frac{3}{2} a_\dagger \|\mathbf{Y}\|_{\infty, J+1} \|\mathbf{Z}\|_{\infty, J+1}. \tag{29}$$

Also, from (27), we have

$$|\mathcal{Q}_h(\mathbf{Y} \cdot \mathbf{Z})| \leq \frac{3}{2} \|\mathbf{Y}\|_{\infty, J+1} \|\mathbf{Z}\|_1. \tag{30}$$

Then, we define the following norm in $\mathcal{X}_h$: for $\mathbf{W}_h = (\mathbf{W}^0, \mathbf{W}^1, \ldots, \mathbf{W}^N) \in \mathcal{X}_h$,

$$\|\mathbf{W}_h\|_{\mathcal{X}_h} = \max_{n=0,\ldots,N} \|\mathbf{W}^n\|_{\infty, J+1}.$$

In addition, in $\mathcal{Y}_h$ we introduce the following norm: for $\mathbf{Z}_h = (\mathbf{Z}^0, \mathbf{Z}_0, \mathbf{Z}_*^1, \ldots, \mathbf{Z}_*^N) \in \mathcal{Y}_k$,

$$\|\mathbf{Z}_h\|_{\mathcal{Y}_k} = \|\mathbf{Z}^0\|_{\infty, J+1} + \|\mathbf{Z}_0\|_{\infty, N} + \sum_{n=1}^{N} h \|\mathbf{Z}_*^n\|_{\infty, J}.$$

For each $h \in H$, the element $\mathbf{u}_h = (\mathbf{u}^0, \mathbf{u}^1, \ldots, \mathbf{u}^N) \in \mathcal{X}_h$ recovers the mesh-grid values of the solution u to (1)-(3): that is, at each time level t^n, $n = 0, 1, \ldots, N$, $\mathbf{u}^n = (u(a_0, t^n), u(a_1, t^n), \ldots, u(a_J, t^n))$. In the same way, $\mathbf{v}_h = (\mathbf{v}^0, \mathbf{v}^1, \ldots, \mathbf{v}^N) \in \mathcal{X}_h$, where $\mathbf{v}^n = (v(a_0, t^n), v(a_1, t^n), \ldots, v(a_J, t^n))$, represents the grid restriction of the solution v to (12)-(14) at each time level t^n, $n = 0, 1, \ldots, N$.

For $h \in H$, let R_h a positive real number, and denote by $\mathcal{B}_{\mathcal{X}_h}(\mathbf{v}_h, R_h) \subset \mathcal{X}_h$, the open ball with center $\mathbf{v}_h$ and radious R_h. Then, we introduce the map $\boldsymbol{\Phi}_h : \mathcal{B}_{\mathcal{X}_h}(\mathbf{v}_h, R_h) \subset \mathcal{X}_h \to \mathcal{Y}_h$ that describes the equations of the discretization proposed to obtain the approximation of v: for $\mathbf{W}_h = (\mathbf{W}^0, \mathbf{W}^1, \ldots, \mathbf{W}^N) \in \mathcal{B}_{\mathcal{X}_h}(\mathbf{v}_h, R_h)$

$$\boldsymbol{\Phi}_h(\mathbf{W}_h) = \mathbf{Z}_h, \tag{31}$$

where $\mathbf{Z}_h = (\mathbf{Z}^0, \mathbf{Z}_0, \mathbf{Z}_*^1, \ldots, \mathbf{Z}_*^N) \in \mathcal{Y}_h$. Each component of $\mathbf{Z}_h$ refers to the residual generated by each part of the discretisation when applied to an element $\mathbf{W}_h$ of the space $\mathcal{X}_h$ to which the numerical approximation $\mathbf{V}_h$ belongs. Thus, $\mathbf{Z}^0 \in \mathbb{R}^{J+1}$ refers to the residual generated by the approximation of the initial data, that is

$$\mathbf{Z}^0 = \mathbf{W}^0 - \mathbf{V}^0, \tag{32}$$

(remember that $\mathbf{V}^0$, is a suitable approximation to the initial condition (14)). The components of $\mathbf{Z}_0 \in \mathbb{R}^N$, that represents the residual in the numerical boundary condition (22), are characterized by

$$Z_0^{n+1} = W_0^{n+1} - \mathcal{Q}_h(\boldsymbol{\Pi} \cdot \boldsymbol{\beta}^{n+1} \cdot \mathbf{W}^{n+1}), \quad n = 0, 1, \ldots, N-1. \tag{33}$$

Finally, for $n = 0, 1, \dots, N-1$, vector $\mathbf{Z}_*^{n+1} \in \mathbb{R}^J$, which relates to the residual generated by the discretisation (21) of the balance law (17), is described by: for $j = 0, 1, \dots, J-1$,

$$Z_{j+1}^{n+1} = \frac{1}{h}\Bigg\{W_{j+1}^{n+1} - W_j^n \exp\Big(-\frac{h}{2}\Big[\mu_b\left(a_j, \mathcal{Q}_h(\boldsymbol{\Pi}\cdot\boldsymbol{\gamma}_\mu\cdot\mathbf{W}^n), t^n\right) + \mu_b\big(a_{j+1}, \mathcal{Q}_h(\boldsymbol{\Pi}\cdot\boldsymbol{\gamma}_\mu\cdot\mathbf{W}^{n+1,*}), t^{n+1}\big)\Big]\Big)\Bigg\}, \tag{34}$$

where we require to compute the auxiliar vectors $\mathbf{W}^{n+1,*}$ defined by: for $j = 0, 1, \dots, J-1$,

$$W_{j+1}^{n+1,*} = W_j^n \exp\big(-h\,\mu_b\left(a_j, \mathcal{Q}_h(\boldsymbol{\Pi}\cdot\boldsymbol{\gamma}_\mu\cdot\mathbf{W}^n), t^n\right)\big), \tag{35}$$

$$W_0^{n+1,*} = \mathcal{Q}_h(\boldsymbol{\Pi}\cdot\boldsymbol{\beta}^{n+1,*}\cdot\mathbf{W}^{n+1,*}), \tag{36}$$

although it should be remembered that the auxiliary value $W_0^{n+1,*}$ is not necessary in the study.

Then $\mathbf{V}_h = (\mathbf{V}^0, \mathbf{V}^1, \dots, \mathbf{V}^N) \in \mathcal{B}_{\mathcal{X}_h}(\mathbf{v}_h, R_h)$, is a solution of the scheme with initial data $\mathbf{V}^0$, and described by equations (19)-(22) if, and only if,

$$\boldsymbol{\Phi}_h(\mathbf{V}_h) = \mathbf{0}.$$

First, a theorem is introduced which establishes that the operator is well-defined for the analysis.

Theorem 1 *Assume the regularity hypotheses (H1)-(H4) on the data functions and the solution $v(a,t)$, and the disposal of approximations to the intrinsic survival probability π_0 that satisfy (H0).*

Considering that $R_h = o(1)$, as $h \to 0$, if $\mathbf{W}_h = (\mathbf{W}^0, \mathbf{W}^1, \dots, \mathbf{W}^N) \in \mathcal{B}_{\mathcal{X}_h}(\mathbf{v}_h, R_h)$ then, for h sufficiently small, and $n = 0, 1, \dots, N$

$$\mathcal{Q}_h(\boldsymbol{\Pi}\cdot\boldsymbol{\gamma}_\mu\cdot\mathbf{W}^n) \in D_\mu\,, \qquad \mathcal{Q}_h(\boldsymbol{\Pi}\cdot\boldsymbol{\gamma}_\beta\cdot\mathbf{W}^n) \in D_\beta\,,$$

and, the auxiliar vectors $\mathbf{W}^{n,*}$, $n = 1, 2, \dots, N$, defined by (35), (36), also satisfy

$$\mathcal{Q}_h(\boldsymbol{\Pi}\cdot\boldsymbol{\gamma}_\mu\cdot\mathbf{W}^{n,*}) \in D_\mu\,.$$

Proof The definition and the convergence property of $\mathcal{Q}_h$ together with (29), the regularity hypotheses assumed and the boundedness of functions, provide, for $n = 0, 1, \dots, N$

$$\begin{aligned}
|\mathcal{Q}_h(\boldsymbol{\Pi}\cdot\boldsymbol{\gamma}_\mu\cdot\mathbf{W}^n) - I_\mu(t^n)| &\le |\mathcal{Q}_h(\boldsymbol{\Pi}\cdot\boldsymbol{\gamma}_\mu\cdot(\mathbf{W}^n - \mathbf{v}^n))| \\
&\quad + |\mathcal{Q}_h((\boldsymbol{\Pi}-\boldsymbol{\pi}_0)\cdot\boldsymbol{\gamma}_\mu\cdot\mathbf{v}^n)| + |\mathcal{Q}_h(\boldsymbol{\pi}_0\cdot\boldsymbol{\gamma}_\mu\cdot\mathbf{v}^n) - I_\mu(t^n)| \\
&\le \frac{3}{2}\,a_\dagger\,\|\boldsymbol{\Pi}\cdot\boldsymbol{\gamma}_\mu\|_{\infty,J+1}\,\|\mathbf{W}^n - \mathbf{v}^n\|_{\infty,J+1} \\
&\quad + \frac{3}{2}\,a_\dagger\,\|\boldsymbol{\gamma}_\mu\cdot\mathbf{v}^n\|_{\infty,J+1}\,\|\boldsymbol{\Pi}-\boldsymbol{\pi}_0\|_{\infty,J+1} + \mathcal{O}(h^2) \\
&\le C\,R_h + \mathcal{O}(h^2).
\end{aligned} \tag{37}$$

From now on, C will denote a positive constant which is independent of h, and possibly has different values in different places.

We can proceed in a similar way to set, for $n = 0, 1, \dots, N$

$$|\mathcal{Q}_h(\boldsymbol{\Pi}\cdot\boldsymbol{\gamma}_\beta\cdot\mathbf{W}^n) - I_\beta(t^n)| \le C\,R_h + \mathcal{O}(h^2). \tag{38}$$

On the other hand, the use of (35) and (17), the Mean Value Theorem, the expression of the error of the rectangle quadrature rule, and (37) allow us to obtain, for $n = 0, 1, \ldots, N-1$, $j = 0, 1, \ldots, J-1$

$$
\begin{aligned}
|W_{j+1}^{n+1,*} - v_{j+1}^{n+1}| &\le |W_j^n - v_j^n| \exp\left(-\int_0^h \mu_b\left(a_j + s, I_\mu(t^n+s), t^n+s\right) ds\right) \\
&\quad + |W_j^n| \Big| \exp\left(-h\,\mu_b\left(a_j, \mathcal{Q}_h(\boldsymbol{\Pi}\cdot\boldsymbol{\gamma}_\mu\cdot\mathbf{W}^n), t^n\right)\right) \\
&\qquad - \exp\left(-\int_0^h \mu_b\left(a_j+s, I_\mu(t^n+s), t^n+s\right) ds\right)\Big| \\
&\le (1+Ch)\,|W_j^n - v_j^n| \\
&\quad + C\left|\int_0^h \mu_b\left(a_j+s, I_\mu(t^n+s), t^n+s\right) ds - h\mu_b\left(a_j, \mathcal{Q}_h(\boldsymbol{\Pi}\cdot\boldsymbol{\gamma}_\mu\cdot\mathbf{W}^n), t^n\right)\right| \\
&\le (1+Ch)\,|W_j^n - v_j^n| \\
&\quad + C\left|\int_0^h \mu_b\left(a_j+s, I_\mu(t^n+s), t^n+s\right) ds - h\mu_b\left(a_j, I_\mu(t^n), t^n\right)\right| \\
&\quad + C\,h\,\left|\mu_b\left(a_j, I_\mu(t^n), t^n\right) - \mu_b\left(a_j, \mathcal{Q}_h(\boldsymbol{\Pi}\cdot\boldsymbol{\gamma}_\mu\cdot\mathbf{W}^n), t^n\right)\right| \\
&\le (1+C\,h)\,|W_j^n - v_j^n| + C\,h\,|I_\mu(t^n) - \mathcal{Q}_h(\boldsymbol{\Pi}\cdot\boldsymbol{\gamma}_\mu\cdot\mathbf{W}^n)| + \mathcal{O}(h^2) \\
&\le (1+C\,h)\,R_h + \mathcal{O}(h^2).
\end{aligned} \tag{39}
$$

Then, note that it is not necessary to bound $|W_0^{n,*} - v_0^n|$ to conclude that, for $n = 1, 2, \ldots, N$,

$$
|\mathbf{W}^{n,*} - \mathbf{v}^n|_{\infty,J+1} \le (1+C\,h)\,R_h + \mathcal{O}(h^2). \tag{40}
$$

Finally, if we use (28), (29) and (40), we have, for $n = 1, 2, \ldots, N$

$$
\begin{aligned}
|\mathcal{Q}_h(\boldsymbol{\Pi}\cdot\boldsymbol{\gamma}_\mu\cdot\mathbf{W}^{n,*}) - I_\mu(t^n)| &\le |\mathcal{Q}_h(\boldsymbol{\Pi}\cdot\boldsymbol{\gamma}_\mu\cdot(\mathbf{W}^{n,*} - \mathbf{v}^n))| \\
&\quad + |\mathcal{Q}_h((\boldsymbol{\Pi} - \boldsymbol{\pi}_0)\cdot\boldsymbol{\gamma}_\mu\cdot\mathbf{v}^n)| + |\mathcal{Q}_h(\boldsymbol{\pi}_0\cdot\boldsymbol{\gamma}_\mu\cdot\mathbf{v}^n) - I_\mu(t^n)| \\
&\le \frac{3}{2}\,a_\dagger\,\|\boldsymbol{\Pi}\cdot\boldsymbol{\gamma}_\mu\|_{\infty,J+1}\,|\mathbf{W}^{n,*} - \mathbf{v}^n|_{\infty,J+1} \\
&\quad + \frac{3}{2}\,a_\dagger\,\|\boldsymbol{\gamma}_\mu\cdot\mathbf{v}^n\|_{\infty,J+1}\,\|\boldsymbol{\Pi} - \boldsymbol{\pi}_0\|_{\infty,J+1} + \mathcal{O}(h^2) \\
&\le C\,(1+h)\,R_h + \mathcal{O}(h^2).
\end{aligned} \tag{41}
$$

We conclude the result taking into account that $R_h = \mathrm{o}(1)$, as $h \to 0$, in (37), (38) and (41). □

Now, we define the *local discretization error* as $\boldsymbol{\Phi}_h(\mathbf{v}_h) \in \mathcal{Y}_h$, and we say that the discretization is *consistent* if $\lim_{h\to 0} \|\boldsymbol{\Phi}_h(\mathbf{v}_h)\|_{\mathcal{Y}_h} = 0$. The following result establishes the consistency of the numerical scheme defined by (31).

Theorem 2 *(Consistency) Assume the regularity hypotheses (H1)-(H4) on the data functions and the solution $v(a,t)$, and the disposal of approximations to the intrinsic survival probability π_0 that satisfy (H0). Then, as $h \to 0$,*

$$
\|\boldsymbol{\Phi}_h(\mathbf{v}_h)\|_{\mathcal{Y}_h} = \|\mathbf{v}^0 - \mathbf{V}^0\|_{\infty,J+1} + \mathcal{O}(h^2). \tag{42}
$$

Proof Let us denote the components of the local discretization error vector as $\boldsymbol{\Phi}_h(\mathbf{v}_h) = (\mathbf{z}^0, \mathbf{z}_0, \mathbf{z}_*^1, \ldots, \mathbf{z}_*^N)$.

Following the steps given in Theorem 1 to obtain (37), but taking $\mathbf{W}^n = \mathbf{v}^n$ (that is, the center of the ball), for $n = 0, 1, \ldots, N$, we conclude that

$$|\mathcal{Q}_h(\boldsymbol{\Pi} \cdot \boldsymbol{\gamma}_\mu \cdot \mathbf{v}^n) - I_\mu(t^n)| = \mathcal{O}(h^2). \tag{43}$$

In a similar way, for $n = 0, 1, \ldots, N$, we can arrive at

$$|\mathcal{Q}_h(\boldsymbol{\Pi} \cdot \boldsymbol{\gamma}_\beta \cdot \mathbf{v}^n) - I_\beta(t^n)| = \mathcal{O}(h^2). \tag{44}$$

From $\mathbf{v}^n$ we define the auxiliar vectors $\mathbf{v}^{n+1,*}$, $n = 0, 1, \ldots, N-1$, with components: for $j = 0, 1 \ldots, J-1$,

$$\begin{aligned} v_{j+1}^{n+1,*} &= v_j^n \, \exp\left(-h \, \mu_b(a_j, \mathcal{Q}_h(\boldsymbol{\Pi} \cdot \boldsymbol{\gamma}_\mu \cdot \mathbf{v}^n), t^n)\right), \\ v_0^{n+1,*} &= \mathcal{Q}_h(\boldsymbol{\Pi} \cdot \boldsymbol{\beta}^{n+1,*} \cdot \mathbf{v}^{n+1,*}), \end{aligned}$$

where $\boldsymbol{\beta}^{n+1,*}$ has components $\beta_j^{n+1,*} = \beta(a_j, \mathcal{Q}_h(\boldsymbol{\Pi} \cdot \boldsymbol{\gamma}_\beta \cdot \mathbf{v}^{n+1,*}), t^{n+1})$, $j = 0, 1, \ldots J$. Then, as in Theorem 1 to get (39) but taking $\mathbf{W}^{n+1,*} = \mathbf{v}^{n+1,*}$, and from (43), we obtain for $n = 0, 1, \ldots, N-1$, $J = 0, 1, \ldots, J-1$,

$$|v_{j+1}^{n+1,*} - v_{j+1}^{n+1}| = \mathcal{O}(h^2),$$

and, therefore

$$|\mathbf{v}^{n+1,*} - \mathbf{v}^{n+1}|_{\infty, J+1} = \mathcal{O}(h^2). \tag{45}$$

Finally, by (45) and following Theorem 1 to set (41), again with $\mathbf{W}^{n,*} = \mathbf{v}^{n,*}$, for $n = 1, 2, \ldots, N$, we have

$$|\mathcal{Q}_h(\boldsymbol{\Pi} \cdot \boldsymbol{\gamma}_\mu \cdot \mathbf{v}^{n,*}) - I_\mu(t^n)| = \mathcal{O}(h^2). \tag{46}$$

Now, we analyze the different vectors that make up the local discretization error $\boldsymbol{\Phi}_h(\mathbf{v}_h)$. First, from (32),

$$\|\mathbf{z}^0\|_{\infty, J+1} = \|\mathbf{v}^0 - \mathbf{V}^0\|_{\infty, J+1}.$$

Next remember (33), and by means of (13), the components of $\mathbf{z}_0$ are, for $n = 0, 1, \ldots, N-1$,

$$z_0^{n+1} = \int_0^{a_\dagger} \pi_0(a) \, \beta(a, I_\beta(t^{n+1}), t^{n+1}) \, v(a, t^{n+1}) \, da - \mathcal{Q}_h(\boldsymbol{\Pi} \cdot \boldsymbol{\beta}^{n+1} \cdot \mathbf{v}^{n+1}),$$

here $\boldsymbol{\beta}^{n+1}$ has components $\beta_j^{n+1} = \beta(a_j, \mathcal{Q}_h(\boldsymbol{\Pi} \cdot \boldsymbol{\gamma}_\beta \cdot \mathbf{v}^{n+1}), t^{n+1})$, $j = 0, 1, \ldots J$. Also, for the sake of simplicity, we define the vector $\boldsymbol{\beta}_I^{n+1}$, with components $\left(\boldsymbol{\beta}_I^{n+1}\right)_j = \beta(a_j, I_\beta(t^{n+1}), t^{n+1})$, $j = 0, 1, \ldots J$, $n = 0, 1, \ldots, N-1$. Then, the smoothness of the solution v and the function β, the convergence property of $\mathcal{Q}_h$, inequality (29), the accuracy of the approximations in $\boldsymbol{\Pi}$, the Mean Value Theorem and the result (44), lead to, for $n = 0, 1, \ldots, N-1$,

$$\begin{aligned} |z_0^{n+1}| \le & \left| \int_0^{a_\dagger} \pi_0(a) \, \beta(a, I_\beta(t^{n+1}), t^{n+1}) \, v(a, t^{n+1}) \, da - \mathcal{Q}_h(\boldsymbol{\pi}_0 \cdot \boldsymbol{\beta}_I^{n+1} \cdot \mathbf{v}^{n+1}) \right| \\ & + \left| \mathcal{Q}_h((\boldsymbol{\pi}_0 - \boldsymbol{\Pi}) \cdot \boldsymbol{\beta}_I^{n+1} \cdot \mathbf{v}^{n+1}) \right| + \left| \mathcal{Q}_h(\boldsymbol{\Pi} \cdot \left(\boldsymbol{\beta}_I^{n+1} - \boldsymbol{\beta}^{n+1}\right) \cdot \mathbf{v}^{n+1}) \right| \end{aligned}$$

$$\leq \frac{3}{2}\, a_\dagger\, \|\boldsymbol{\beta}_I^{n+1} \cdot \mathbf{v}^{n+1}\|_{\infty,J+1}\, \|\boldsymbol{\pi}_0 - \boldsymbol{\Pi}\|_{\infty,J+1}$$
$$+\frac{3}{2}\, a_\dagger\, \|\boldsymbol{\Pi} \cdot \mathbf{v}^{n+1}\|_{\infty,J+1}\, \|\boldsymbol{\beta}_I^{n+1} - \boldsymbol{\beta}^{n+1}\|_{\infty,J+1} + \mathcal{O}(h^2)$$
$$\leq C\, |I_\beta(t^{n+1}) - \mathcal{Q}_h(\boldsymbol{\Pi} \cdot \boldsymbol{\gamma}_\beta \cdot \mathbf{v}^{n+1})| + \mathcal{O}(h^2) = \mathcal{O}(h^2),$$

and then, $\|\mathbf{z}_0\|_{\infty,N} = \mathcal{O}(h^2)$.

To end, when $n = 0, 1, \ldots, N-1$, from (34) and using (17), we can write the components of $\mathbf{z}_*^{n+1}$ as, for $j = 0, 1, \ldots, J-1$,

$$z_{j+1}^{n+1} = \frac{1}{h}\, v_j^n \left\{ \exp\left(-\int_0^h \mu_b\left(a_j + s, I_\mu(t^n + s), t^n + s\right) ds \right) \right.$$
$$- \exp\left(-\frac{h}{2} \left[\mu_b\left(a_j, \mathcal{Q}_h(\boldsymbol{\Pi} \cdot \boldsymbol{\gamma}_\mu \cdot \mathbf{v}^n), t^n\right) \right.\right.$$
$$\left.\left.\left. + \mu_b\left(a_{j+1}, \mathcal{Q}_h(\boldsymbol{\Pi} \cdot \boldsymbol{\gamma}_\mu \cdot \mathbf{v}^{n+1,*}), t^{n+1}\right)\right]\right)\right\}.$$

Then, again, the boundedness of the function μ_b and the solution v, the Mean Value Theorem, the expression of the error of the trapezoidal quadrature rule, and inequalities (43) and (46) leads to

$$|z_{j+1}^{n+1}| \leq \frac{C}{h} \left| \frac{h}{2}\left[\mu_b\left(a_j, \mathcal{Q}_h(\boldsymbol{\Pi}\cdot\boldsymbol{\gamma}_\mu\cdot\mathbf{v}^n), t^n\right) + \mu_b\left(a_{j+1}, \mathcal{Q}_h(\boldsymbol{\Pi}\cdot\boldsymbol{\gamma}_\mu\cdot\mathbf{v}^{n+1,*}), t^{n+1}\right)\right] \right.$$
$$\left. - \int_0^h \mu_b\left(a_j + s, I_\mu(t^n + s), t^n + s\right) ds \right|$$
$$\leq \frac{C}{2}\, \left|\mu_b\left(a_j, \mathcal{Q}_h(\boldsymbol{\Pi} \cdot \boldsymbol{\gamma}_\mu \cdot \mathbf{v}^n), t^n\right) - \mu_b\left(a_j, I_\mu(t^n), t^n\right)\right|$$
$$+\frac{C}{2}\, \left|\mu_b\left(a_{j+1}, \mathcal{Q}_h(\boldsymbol{\Pi} \cdot \boldsymbol{\gamma}_\mu \cdot \mathbf{v}^{n+1,*}), t^{n+1}\right) - \mu_b\left(a_{j+1}, I_\mu(t^{n+1}), t^{n+1}\right)\right|$$
$$+\frac{C}{h} \left| \frac{h}{2}\, \left[\mu_b\left(a_j, I_\mu(t^n), t^n\right) + \mu_b\left(a_{j+1}, I_\mu(t^{n+1}), t^{n+1}\right)\right] \right.$$
$$\left. - \int_0^h \mu_b(a_j + s, I_\mu(t^n + s), t^n + s) ds \right|$$
$$\leq C\big(|\mathcal{Q}_h(\boldsymbol{\Pi}\cdot \boldsymbol{\gamma}_\mu\cdot \mathbf{v}^n) - I_\mu(t^n)| + |\mathcal{Q}_h(\boldsymbol{\Pi}\cdot\boldsymbol{\gamma}_\mu\cdot\mathbf{v}^{n+1,*}) - I_\mu(t^{n+1})|\big) + \mathcal{O}(h^2)$$
$$= \mathcal{O}(h^2),$$

Thus, $\|\mathbf{z}_*^{n+1}\|_{\infty,J} = \mathcal{O}(h^2)$, $0 \leq n \leq N-1$, and (42) is proved. □

Next, we introduce the *stability with h-dependent thresholds*. For $h \in H$, let R_h a real number (*the stability threshold*) with $0 < R_h < \infty$: we say that the discretization (31) is stable for $\mathbf{v}_h$ restricted to the threshold R_h, if there exist two positive constants h_0 and S (*the stability constant*) such that, for any $h \in H$ with $h \leq h_0$, the open ball $\mathcal{B}_{\mathcal{X}_h}(\mathbf{v}_h, R_h) \subset \mathcal{X}_h$ is in the domain of $\boldsymbol{\Phi}_h$, and for $\mathbf{W}_h, \mathbf{P}_h \in \mathcal{B}_{\mathcal{X}_h}(\mathbf{v}_h, R_h)$

$$\|\mathbf{W}_h - \mathbf{P}_h\|_{\mathcal{X}_h} \leq S\, \|\boldsymbol{\Phi}_h(\mathbf{W}_h) - \boldsymbol{\Phi}_h(\mathbf{P}_h)\|_{\mathcal{Y}_h}.$$

Theorem 3 *(Stability) Assume the regularity hypotheses (H1)-(H4) on the data functions and the solution $v(a, t)$, and the disposal of approximations to the intrinsic survival probability π_0 that satisfy (H0). Then the discretization is stable for $\mathbf{v}_h$ with thresholds $R_h = R\, h$.*

Proof Since $R_h = R\, h = o(1)$, as $h \to 0$, Theorem 1 assures that $\boldsymbol{\Phi}_h$ is well-defined over $\mathcal{B}_{\mathcal{X}_h}(\mathbf{v}_h, R_h)$, for h small enough. Then, for $\mathbf{W}_h = (\mathbf{W}^0, \mathbf{W}^1, \ldots, \mathbf{W}^N)$ and $\mathbf{P}_h = (\mathbf{P}^0, \mathbf{P}^1, \ldots, \mathbf{P}^N)$ in $\mathcal{B}_{\mathcal{X}_h}(\mathbf{v}_h, R_h)$, we denote, respectively, $\mathbf{Z}_h = \boldsymbol{\Phi}_h(\mathbf{W}_h) = (\mathbf{Z}^0, \mathbf{Z}_0, \mathbf{Z}^1_*, \ldots, \mathbf{Z}^N_*)$, and $\mathbf{S}_h = \boldsymbol{\Phi}_h(\mathbf{P}_h) = (\mathbf{S}^0, \mathbf{S}_0, \mathbf{S}^1_*, \ldots, \mathbf{S}^N_*)$.

First of all, we make some remarks on the notation. On the one hand, note that the components of $\mathbf{Z}_0$ and $\mathbf{S}_0$ are defined as in (33). However, in order to avoid any confusion, we write, for $n = 0, 1, \ldots, N-1$,

$$Z_0^{n+1} = W_0^{n+1} - \mathcal{Q}_h(\boldsymbol{\Pi} \cdot \boldsymbol{\beta}_W^{n+1} \cdot \mathbf{W}^{n+1}), \tag{47}$$

$$S_0^{n+1} = P_0^{n+1} - \mathcal{Q}_h(\boldsymbol{\Pi} \cdot \boldsymbol{\beta}_P^{n+1} \cdot \mathbf{P}^{n+1}), \tag{48}$$

where $\boldsymbol{\beta}_W^{n+1}$ and $\boldsymbol{\beta}_P^{n+1}$, represent the vectors with components defined by $\left(\boldsymbol{\beta}_W^{n+1}\right)_j = \beta(a_j, \mathcal{Q}_h(\boldsymbol{\Pi} \cdot \boldsymbol{\gamma}_\beta \cdot \mathbf{W}^{n+1}), t^{n+1})$ and $\left(\boldsymbol{\beta}_P^{n+1}\right)_j = \beta(a_j, \mathcal{Q}_h(\boldsymbol{\Pi} \cdot \boldsymbol{\gamma}_\beta \cdot \mathbf{P}^{n+1}), t^{n+1})$, $j = 0, 1, \ldots, J$, $n = 0, 1, \ldots, N-1$, respectively.

On the other hand, for $n = 0, 1 \ldots, N-1$, we define as in (35), (36) the auxiliar vectors $\mathbf{W}^{n+1,*}$ and $\mathbf{P}^{n+1,*}$ with components: for $j = 0, 1, \ldots, J-1$,

$$W_{j+1}^{n+1,*} = W_j^n \exp\left(-h\, \mu_b\left(a_j, \mathcal{Q}_h(\boldsymbol{\Pi} \cdot \boldsymbol{\gamma}_\mu \cdot \mathbf{W}^n), t^n\right)\right), \tag{49}$$
$$W_0^{n+1,*} = \mathcal{Q}_h(\boldsymbol{\Pi} \cdot \boldsymbol{\beta}_W^{n+1,*} \cdot \mathbf{W}^{n+1,*}),$$
$$P_{j+1}^{n+1,*} = P_j^n \exp\left(-h\, \mu_b\left(a_j, \mathcal{Q}_h(\boldsymbol{\Pi} \cdot \boldsymbol{\gamma}_\mu \cdot \mathbf{P}^n), t^n\right)\right),$$
$$P_0^{n+1,*} = \mathcal{Q}_h(\boldsymbol{\Pi} \cdot \boldsymbol{\beta}_P^{n+1,*} \cdot \mathbf{P}^{n+1,*}), \tag{50}$$

where $\boldsymbol{\beta}_{\boldsymbol{W}}^{n+1,*}$ and $\boldsymbol{\beta}_{\boldsymbol{P}}^{n+1,*}$ are the vectors with components defined by $\left(\boldsymbol{\beta}_W^{n+1,*}\right)_j = \beta(a_j, \mathcal{Q}_h(\boldsymbol{\Pi} \cdot \boldsymbol{\gamma}_\beta \cdot \mathbf{W}^{n+1,*}), t^{n+1})$, and $\left(\boldsymbol{\beta}_P^{n+1,*}\right)_j = \beta(a_j, \mathcal{Q}_h(\boldsymbol{\Pi} \cdot \boldsymbol{\gamma}_\beta \cdot \mathbf{P}^{n+1,*}), t^{n+1})$, $j = 0, 1, \ldots, J$, respectively.

We set $\mathbf{E}^n = \mathbf{W}^n - \mathbf{P}^n$, $n = 0, 1, \ldots, N$, and $\mathbf{E}^{n+1,*} = \mathbf{W}^{n+1,*} - \mathbf{P}^{n+1,*}$, $n = 0, 1, \ldots, N-1$, and initially we are going to bound $\|\mathbf{E}^n\|_1$, and then $\|\mathbf{E}^n\|_{\infty,J+1}$.

To this end, we obtain some preliminary bounds. From the regularity of the functions, using the Mean Value Theorem and (30), for $n = 1, 2, \ldots, N$, $j = 0, 1, \ldots, J$, we have

$$\left|\left(\boldsymbol{\beta}_W^n\right)_j - \left(\boldsymbol{\beta}_P^n\right)_j\right| \le C|\mathcal{Q}_h(\boldsymbol{\Pi} \cdot \boldsymbol{\gamma}_\beta \cdot \mathbf{E}^n)| \le \frac{3}{2}\, C\, \|\boldsymbol{\Pi} \cdot \boldsymbol{\gamma}_\beta\|_{\infty,J+1} \|\mathbf{E}^n\|_1,$$

and then

$$\|\boldsymbol{\beta}_W^n - \boldsymbol{\beta}_P^n\|_{\infty,J+1} \le C\, \|\mathbf{E}^n\|_1. \tag{51}$$

Also, from (49), (50), if we employ the regularity hypotheses, boundedness of $\mathbf{P}_h$, the Mean Value Theorem and (30), for $n = 0, 1, \ldots, N-1$, $j = 0, 1, \ldots, J-1$, we arrive at

$$\begin{aligned} |E_{j+1}^{n+1,*}| &= |W_{j+1}^{n+1,*} - P_{j+1}^{n+1,*}| \\ &\le |E_j^n| \exp\left(-h\, \mu_b\left(a_j, \mathcal{Q}_h(\boldsymbol{\Pi} \cdot \boldsymbol{\gamma}_\mu \cdot \mathbf{W}^n), t^n\right)\right) \\ &\quad + |P_j^n|\, \Big| \exp\left(-h\, \mu_b\left(a_j, \mathcal{Q}_h(\boldsymbol{\Pi} \cdot \boldsymbol{\gamma}_\mu \cdot \mathbf{W}^n), t^n\right)\right) \\ &\qquad - \exp\left(-h\, \mu_b\left(a_j, \mathcal{Q}_h(\boldsymbol{\Pi} \cdot \boldsymbol{\gamma}_\mu \cdot \mathbf{P}^n), t^n\right)\right)\Big| \end{aligned}$$

$$\begin{aligned}
&\leq (1 + C\,h)\,|E_j^n| + C\,h\,\Big|\mu_b\left(a_j, \mathcal{Q}_h(\boldsymbol{\Pi}\cdot\boldsymbol{\gamma}_\mu\cdot\mathbf{W}^n), t^n\right)\\
&\qquad\qquad -\mu_b\left(a_j, \mathcal{Q}_h(\boldsymbol{\Pi}\cdot\boldsymbol{\gamma}_\mu\cdot\mathbf{P}^n), t^n\right)\Big|\\
&\leq (1 + C\,h)\,|E_j^n| + C\,h\,|\mathcal{Q}_h(\boldsymbol{\Pi}\cdot\boldsymbol{\gamma}_\mu\cdot\mathbf{E}^n)|\\
&\leq (1 + C\,h)\,|E_j^n| + \frac{3}{2}C\,h\,\|\boldsymbol{\Pi}\cdot\boldsymbol{\gamma}_\mu\|_{\infty,J+1}\|\mathbf{E}^n\|_1.
\end{aligned}$$

As a consequence,

$$\begin{aligned}
|\mathbf{E}^{n+1,*}|_1 &= \sum_{j=1}^{J} h\,|E_j^{n+1,*}|\\
&\leq (1 + C\,h)\sum_{j=1}^{J} h\,|E_{j-1}^n| + C\,h\,a_\dagger\,\|\mathbf{E}^n\|_1 \leq (1 + C\,h)\,\|\mathbf{E}^n\|_1.
\end{aligned}\tag{52}$$

For $n = 0$, from the definition of vectors $\mathbf{Z}^0$ and $\mathbf{S}^0$ as in (32), we have

$$\mathbf{E}^0 = \mathbf{W}^0 - \mathbf{P}^0 = \left(\mathbf{Z}^0 + \mathbf{V}^0\right) - \left(\mathbf{S}^0 + \mathbf{V}^0\right) = \mathbf{Z}^0 - \mathbf{S}^0. \tag{53}$$

For $n = 1, 2, \ldots, N$, on the one hand, the expressions (47) and (48) describing $\mathbf{Z}_0$ and $\mathbf{S}_0$, respectively, bounds (30), (29), the regularity hypotheses and (51), gives

$$\begin{aligned}
|E_0^n| &= |W_0^n - P_0^n| \leq |Z_0^n - S_0^n| + |\mathcal{Q}_h(\boldsymbol{\Pi}\cdot\boldsymbol{\beta}_W^n\cdot\mathbf{W}^n) - \mathcal{Q}_h(\boldsymbol{\Pi}\cdot\boldsymbol{\beta}_P^n\cdot\mathbf{P}^n)|\\
&\leq |Z_0^n - S_0^n| + |\mathcal{Q}_h(\boldsymbol{\Pi}\cdot\boldsymbol{\beta}_W^n\cdot\mathbf{E}^n)| + |\mathcal{Q}_h(\boldsymbol{\Pi}\cdot(\boldsymbol{\beta}_W^n - \boldsymbol{\beta}_P^n)\cdot\mathbf{P}^n)|\\
&\leq |Z_0^n - S_0^n| + \frac{3}{2}\,\|\boldsymbol{\Pi}\cdot\boldsymbol{\beta}_W^n\|_{\infty,J+1}\,\|\mathbf{E}^n\|_1\\
&\quad + \frac{3}{2}\,a_\dagger\,\|\boldsymbol{\Pi}\cdot\mathbf{P}^n\|_{\infty,J+1}\|\boldsymbol{\beta}_W^n - \boldsymbol{\beta}_P^n\|_{\infty,J+1}\\
&\leq C\,\|\mathbf{E}^n\|_1 + |Z_0^n - S_0^n|.
\end{aligned}\tag{54}$$

On the other hand, from (34) that describes the components of vectors $\mathbf{Z}_*^{n+1}$ and $\mathbf{S}_*^{n+1}$, $n = 0, 1, \ldots, N-1$, using the regularity hypotheses and the boundedness of $\mathbf{P}_h$, the Mean Value Theorem, and the bounds (30) and (27), we obtain, for $j = 0, 1, \ldots, J-1$

$$\begin{aligned}
|E_{j+1}^{n+1}| &= |W_{j+1}^{n+1} - P_{j+1}^{n+1}|\\
&\leq h\,|Z_{j+1}^{n+1} - S_{j+1}^{n+1}|\\
&\quad + \Bigg|W_j^n\,\exp\Bigg(-\frac{h}{2}\Big[\mu_b\left(a_j, \mathcal{Q}_h(\boldsymbol{\Pi}\cdot\boldsymbol{\gamma}_\mu\cdot\mathbf{W}^n), t^n\right)\\
&\qquad\qquad + \mu_b\left(a_{j+1}, \mathcal{Q}_h(\boldsymbol{\Pi}\cdot\boldsymbol{\gamma}_\mu\cdot\mathbf{W}^{n+1,*}), t^{n+1}\right)\Big]\Bigg)\\
&\qquad - P_j^n\,\exp\Bigg(-\frac{h}{2}\Big[\mu_b\left(a_j, \mathcal{Q}_h(\boldsymbol{\Pi}\cdot\boldsymbol{\gamma}_\mu\cdot\mathbf{P}^n), t^n\right)\\
&\qquad\qquad + \mu_b\left(a_{j+1}, \mathcal{Q}_h(\boldsymbol{\Pi}\cdot\boldsymbol{\gamma}_\mu\cdot\mathbf{P}^{n+1,*}), t^{n+1}\right)\Big]\Bigg)\Bigg|\\
&\leq h\,|Z_{j+1}^{n+1} - S_{j+1}^{n+1}|
\end{aligned}$$

$$
\begin{aligned}
&+|E_j^n| \exp\left(-\frac{h}{2}\left[\mu_b\left(a_j, \mathcal{Q}_h(\boldsymbol{\Pi}\cdot\boldsymbol{\gamma}_\mu\cdot\mathbf{W}^n), t^n\right)\right.\right.\\
&\qquad\qquad\left.\left.+\mu_b\left(a_{j+1}, \mathcal{Q}_h(\boldsymbol{\Pi}\cdot\boldsymbol{\gamma}_\mu\cdot\mathbf{W}^{n+1,*}), t^{n+1}\right)\right]\right)\\
&+|P_j^n| \left|\exp\left(-\frac{h}{2}\left[\mu_b\left(a_j, \mathcal{Q}_h(\boldsymbol{\Pi}\cdot\boldsymbol{\gamma}_\mu\cdot\mathbf{W}^n), t^n\right)\right.\right.\right.\\
&\qquad\qquad\left.\left.+\mu_b\left(a_{j+1}, \mathcal{Q}_h(\boldsymbol{\Pi}\cdot\boldsymbol{\gamma}_\mu\cdot\mathbf{W}^{n+1,*}), t^{n+1}\right)\right]\right)\\
&\qquad-\exp\left(-\frac{h}{2}\left[\mu_b\left(a_j, \mathcal{Q}_h(\boldsymbol{\Pi}\cdot\boldsymbol{\gamma}_\mu\cdot\mathbf{P}^n), t^n\right)\right.\right.\\
&\qquad\qquad\left.\left.\left.+\mu_b\left(a_{j+1}, \mathcal{Q}_h(\boldsymbol{\Pi}\cdot\boldsymbol{\gamma}_\mu\cdot\mathbf{P}^{n+1,*}), t^{n+1}\right)\right]\right)\right|\\
&\le h\,|Z_{j+1}^{n+1}-S_{j+1}^{n+1}| + (1+C\,h)\,|E_j^n|\\
&\quad+C\,\frac{h}{2}\left|\mu_b\left(a_j, \mathcal{Q}_h(\boldsymbol{\Pi}\cdot\boldsymbol{\gamma}_\mu\cdot\mathbf{W}^n), t^n\right)-\mu_b\left(a_j, \mathcal{Q}_h(\boldsymbol{\Pi}\cdot\boldsymbol{\gamma}_\mu\cdot\mathbf{P}^n), t^n\right)\right|\\
&\quad+C\,\frac{h}{2}\left|\mu_b\left(a_{j+1}, \mathcal{Q}_h(\boldsymbol{\Pi}\cdot\boldsymbol{\gamma}_\mu\cdot\mathbf{W}^{n+1,*}), t^{n+1}\right)\right.\\
&\qquad\left.-\mu_b\left(a_{j+1}, \mathcal{Q}_h(\boldsymbol{\Pi}\cdot\boldsymbol{\gamma}_\mu\cdot\mathbf{P}^{n+1,*}), t^{n+1}\right)\right|\\
&\le h\,|Z_{j+1}^{n+1}-S_{j+1}^{n+1}| + (1+C\,h)\,|E_j^n|\\
&\quad+C\,h\,|\mathcal{Q}_h(\boldsymbol{\Pi}\cdot\boldsymbol{\gamma}_\mu\cdot\mathbf{E}^n)| + C\,h\,|\mathcal{Q}_h(\boldsymbol{\Pi}\cdot\boldsymbol{\gamma}_\mu\cdot\mathbf{E}^{n+1,*})|\\
&\le h\,|Z_{j+1}^{n+1}-S_{j+1}^{n+1}| + (1+C\,h)\,|E_j^n|\\
&\quad+\frac{3}{2}\,C\,h\,\|\boldsymbol{\Pi}\cdot\boldsymbol{\gamma}_\mu\|_{\infty,J+1}\left(\|\mathbf{E}^n\|_1 + |\mathbf{E}^{n+1,*}|_1\right).
\end{aligned}
$$

Finally, by using inequality (52), we can write, for $n = 1, 2, \ldots, N$, $j = 1, 2, \ldots, J$,

$$|E_j^n| \le (1+C\,h)\,|E_{j-1}^{n-1}| + C\,h\,\|\mathbf{E}^{n-1}\|_1 + h\,|Z_j^n - S_j^n|,$$

and, by a recursive reasoning, we conclude that: if $1 \le j < n \le N$, then

$$
\begin{aligned}
|E_j^n| \le (1+C\,h)^j\,|E_0^{n-j}| &+ C\,h\sum_{l=n-j}^{n-1}(1+C\,h)^{n-1-l}\,\|\mathbf{E}^l\|_1\\
&+h\sum_{l=n-j+1}^{n}(1+C\,h)^{n-l}\,|Z_{j-n+l}^l - S_{j-n+l}^l|,
\end{aligned}
\tag{55}
$$

but if $1 \le n \le j \le J$, then

$$
\begin{aligned}
|E_j^n| \le (1+C\,h)^n\,|E_{j-n}^0| &+ C\,h\sum_{l=0}^{n-1}(1+C\,h)^{n-1-l}\|\mathbf{E}^l\|_1\\
&+h\sum_{l=1}^{n}(1+C\,h)^{n-l}\,|Z_{j-n+l}^l - S_{j-n+l}^l|.
\end{aligned}
\tag{56}
$$

Now, we obtain the following bound of the discrete $\mathcal{L}_1$ norm of $\mathbf{E}^n$, $n = 1, 2, \ldots, N$, by a recursive way. Note that it is necessary to distinguish the case $n > J$, which does not involve any component of $\mathbf{E}^0$, from opposite case, which does. In the following, in order to unify both situations, we will assume that the sum having an initial index strictly greater than the final one does not describe any summand.

From (55), (56) and (54)

$$
\begin{aligned}
\|\mathbf{E}^n\|_1 &= \sum_{j=0}^{J} h\,|E_j^n| = h\,|E_0^n| + \sum_{j=1}^{\min\{n-1,J\}} h\,|E_j^n| + \sum_{j=\min\{n-1,J\}+1}^{J} h\,|E_j^n| \\
&\le h\,|E_0^n| \\
&\quad + \sum_{j=1}^{\min\{n-1,J\}} h\,(1+C\,h)^j |E_0^{n-j}| \\
&\quad + \sum_{j=1}^{\min\{n-1,J\}} h \left\{ C\,h \sum_{l=n-j}^{n-1} (1+C\,h)^{n-1-l} \|\mathbf{E}^l\|_1 \right. \\
&\qquad\qquad \left. + h \sum_{l=n-j+1}^{n} (1+C\,h)^{n-l} |Z_{j-n+l}^l - S_{j-n+l}^l| \right\} \\
&\quad + \sum_{j=\min\{n-1,J\}+1}^{J} h\,(1+C\,h)^n\,|E_{j-n}^0| \\
&\quad + \sum_{j=\min\{n-1,J\}+1}^{J} h \left\{ C\,h \sum_{l=0}^{n-1} (1+C\,h)^{n-1-l} \|\mathbf{E}^l\|_1 \right. \\
&\qquad\qquad \left. + h \sum_{l=1}^{n} (1+C\,h)^{n-l} |Z_{j-n+l}^l - S_{j-n+l}^l| \right\} \\
&\le \sum_{j=0}^{\min\{n-1,J\}} h\,(1+C\,h)^j \left\{ C\,\|\mathbf{E}^{n-j}\|_1 + |Z_0^{n-j} - S_0^{n-j}| \right\} \\
&\quad + \sum_{j=\min\{n-1,J\}+1}^{J} h\,(1+C\,h)^n\,|E_{j-n}^0| \\
&\quad + \sum_{j=1}^{\min\{n-1,J\}} C\,h^2 \left\{ \sum_{l=n-j}^{n-1} (1+C\,h)^{n-1-l} \|\mathbf{E}^l\|_1 \right\} \\
&\quad + \sum_{j=\min\{n-1,J\}+1}^{J} C\,h^2 \left\{ \sum_{l=0}^{n-1} (1+C\,h)^{n-1-l} \|\mathbf{E}^l\|_1 \right\} \\
&\quad + \sum_{j=1}^{\min\{n-1,J\}} h^2 \left\{ \sum_{l=n-j+1}^{n} (1+C\,h)^{n-l} |Z_{j-n+l}^l - S_{j-n+l}^l| \right\} \\
&\quad + \sum_{j=\min\{n-1,J\}+1}^{J} h^2 \left\{ \sum_{l=1}^{n} (1+C\,h)^{n-l} |Z_{j-n+l}^l - S_{j-n+l}^l| \right\}
\end{aligned}
$$

$$
\begin{aligned}
&= \sum_{j=\min\{n-1,J\}+1}^{J} h\,(1+C\,h)^n\,|E^0_{j-n}| \\
&\quad + \sum_{j=0}^{\min\{n-1,J\}} C\,h\,(1+C\,h)^j\,\|\mathbf{E}^{n-j}\|_1 \\
&\quad + \sum_{l=\max\{n-J,0\}}^{n-1} C\,h^2 \left\{ \sum_{j=n-l}^{J} (1+C\,h)^{n-1-l}\,\|\mathbf{E}^l\|_1 \right\} \\
&\quad + \sum_{j=0}^{\min\{n-1,J\}} h\,(1+C\,h)^j\,|Z_0^{n-j} - S_0^{n-j}| \\
&\quad + \sum_{l=\max\{n-J,0\}+1}^{n} h^2 \left\{ \sum_{j=n+1-l}^{J} (1+C\,h)^{n-l}\,|Z^l_{j-n+l} - S^l_{j-n+l}| \right\} \\
&\le \sum_{j=\min\{J-n+1,0\}}^{J-n} C\,h\,|E^0_j| \\
&\quad + \sum_{l=\max\{n-J,1\}}^{n} C\,h\,\|\mathbf{E}^l\|_1 + \sum_{l=\max\{n-J,0\}}^{n-1} C\,h \left\{ \sum_{j=1}^{J-n+l+1} h\,\|\mathbf{E}^l\|_1 \right\} \\
&\quad + \sum_{l=\max\{n-J,1\}}^{n} C\,h\,|Z_0^l - S_0^l| + \sum_{l=\max\{n-J,0\}+1}^{n} C\,h \left\{ \sum_{j=1}^{J-n+l} h\,|Z^l_j - S^l_j| \right\} \\
&\le \sum_{j=0}^{J} C\,h\,|E^0_j| + \sum_{l=1}^{n} C\,h\,\|\mathbf{E}^l\|_1 + \sum_{l=0}^{n-1} C\,h \left\{ \sum_{j=1}^{J} h\,\|\mathbf{E}^l\|_1 \right\} \\
&\quad + \sum_{l=1}^{n} C\,h\,|Z_0^l - S_0^l| + \sum_{l=1}^{n} C\,h \left\{ \sum_{j=1}^{J} h\,|Z^l_j - S^l_j| \right\} \\
&\le C \sum_{j=0}^{J} h\,|E^0_j| + C\,h \sum_{l=1}^{n} \|\mathbf{E}^l\|_1 + C\,h\,(J\,h) \sum_{l=0}^{n-1} \|\mathbf{E}^l\|_1 \\
&\quad + C\,(n\,h) \max_{l=1,\ldots n} |Z_0^l - S_0^l| + C\,h\,(J\,h) \sum_{l=1}^{n} \|\mathbf{Z}^l_* - \mathbf{S}^l_*\|_{\infty,J}.
\end{aligned}
$$

As a conclusion, for $n = 1, 2, \ldots, N$,

$$
\|\mathbf{E}^n\|_1 \le Ch \sum_{l=0}^{n} \|\mathbf{E}^l\|_1 + C\,\|\mathbf{E}^0\|_1 + \|\mathbf{Z}_0 - \mathbf{S}_0\|_{\infty,N} + C \sum_{l=1}^{N} h\,\|\mathbf{Z}^l_* - \mathbf{S}^l_*\|_{\infty,J}, \tag{57}
$$

and, for h sufficiently small, by means of the Gronwall discrete lemma in (57), and due to (53) and the relation (25) between the two norms being used, for $n = 0, 1, \ldots, N$, we arrive at

$$
\|\mathbf{E}^n\|_1 \le C\,\|\mathbf{E}^0\|_1 + C\,\|\mathbf{Z}_0 - \mathbf{S}_0\|_{\infty,N} + C \sum_{l=1}^{N} h\,\|\mathbf{Z}^l_* - \mathbf{S}^l_*\|_{\infty,J}
$$

$$
\begin{aligned}
&\leq C \left\{ \|\mathbf{Z}^0 - \mathbf{S}^0\|_{\infty, J+1} + \|\mathbf{Z}_0 - \mathbf{S}_0\|_{\infty, N} + \sum_{l=1}^{N} h \, \|\mathbf{Z}_*^l - \mathbf{S}_*^l\|_{\infty, J} \right\} \\
&= C \, \|\mathbf{Z}_h - \mathbf{S}_h\|_{\mathcal{Y}_h}.
\end{aligned} \tag{58}
$$

Next, we establish a similar bound of the discrete $\mathcal{L}_\infty$ norm of $\mathbf{E}^n$, $n = 0, 1, \ldots, N$. On the one hand, at the left boundary grid point we employ (58) in (54) to also conclude that, for $n = 1, 2, \ldots, N$

$$
\begin{aligned}
|E_0^n| &\leq C \, \|\mathbf{E}^n\|_1 + |Z_0^n - S_0^n| \\
&\leq C \, \|\mathbf{Z}_h - \mathbf{S}_h\|_{\mathcal{Y}_h} + \|\mathbf{Z}_0 - \mathbf{S}_0\|_{\infty, N} \leq C \, \|\mathbf{Z}_h - \mathbf{S}_h\|_{\mathcal{Y}_h}.
\end{aligned} \tag{59}
$$

On the other hand, we consider the inner grid points. If $1 \leq j < n \leq N$, using (55), (59), and (58), we arrive at

$$
\begin{aligned}
|E_j^n| &\leq C \, |E_0^{n-j}| + C \sum_{l=n-j}^{n-1} h \, \|\mathbf{E}^l\|_1 + C \sum_{l=n-j+1}^{n} h \, |Z_{j-n+l}^l - S_{j-n+l}^l| \\
&\leq C \, \|\mathbf{Z}_h - \mathbf{S}_h\|_{\mathcal{Y}_h} + C \, (J \, h) \, \|\mathbf{Z}_h - \mathbf{S}_h\|_{\mathcal{Y}_h} + C \sum_{l=1}^{N} h \, \|\mathbf{Z}_*^l - \mathbf{S}_*^l\|_{\infty, J}.
\end{aligned}
$$

Now, if $1 \leq n \leq j \leq J$, using (56), (53) and (58),

$$
\begin{aligned}
|E_j^n| &\leq C \, |E_{j-n}^0| + C \sum_{l=0}^{n-1} h \, \|\mathbf{E}^l\|_1 + C \sum_{l=1}^{n} h \, |Z_{j-n+l}^l - S_{j-n+l}^l| \\
&\leq C \, \|\mathbf{Z}^0 - \mathbf{S}^0\|_{\infty, J+1} + C \, (J \, h) \, \|\mathbf{Z}_h - \mathbf{S}_h\|_{\mathcal{Y}_h} + C \sum_{l=1}^{N} h \, \|\mathbf{Z}_*^l - \mathbf{S}_*^l\|_{\infty, J}.
\end{aligned}
$$

In any case, for $n = 1, 2, \ldots, N$, $j = 1, 2, \ldots, J$, we can write

$$
|E_j^n| \leq C \, \|\mathbf{Z}_h - \mathbf{S}_h\|_{\mathcal{Y}_h}, \tag{60}
$$

In conclusion, from (59) and (60), $n = 0, 1, \ldots, N$, it yields

$$
\|\mathbf{E}^n\|_{\infty, J+1} \leq C \, \|\mathbf{Z}_h - \mathbf{S}_h\|_{\mathcal{Y}_h},
$$

that proofs the stability. □

Finally, we compare the solution of the differential problem with its numerical approximation. To this end, we define the *global discretization error* as

$$
\mathbf{e}_h = \mathbf{v}_h - \mathbf{V}_h \in \mathcal{X}_h,
$$

and we say that the discretization is *convergent* if there exists $h_0 > 0$ such that for each $h \in H$, with $h \leq h_0$, the numerical method has a solution $\mathbf{V}_h$, and

$$
\lim_{h \to 0} \|\mathbf{e}_h\|_{\mathcal{X}_h} = 0.
$$

To derive the existence and convergence of numerical solutions of (19)-(22) to the solution of problem (12)-(14), we use the following result of the general discretization framework introduced in [18]:

Theorem 4 *(J.C. López-Marcos & J.M. Sanz-Serna, 1985) Assume that the discretization* $\boldsymbol{\Phi}_h$ *is consistent and stable for* $\mathbf{v}_h$ *restricted to the threshold* R_h*. If* $\boldsymbol{\Phi}_h$ *is continuous in* $\mathcal{B}_{\mathcal{X}_h}(\mathbf{v}_h, R_h)$ *and* $\|\boldsymbol{\Phi}_h(\mathbf{v}_h)\|_{\mathcal{Y}_h} = o(R_h)$ *as* $h \to 0$*, then*

1. *for h sufficiently small, the discrete equations* $\boldsymbol{\Phi}_h(\mathbf{V}_h) = \mathbf{0}$ *posses a unique solution in* $\mathcal{B}_{\mathcal{X}_h}(\mathbf{v}_h, R_h)$*,*
2. *as* $h \to 0$*, the numerical solutions converge, and* $\|\mathbf{e}_h\|_{\mathcal{X}_h} = \mathcal{O}(\|\boldsymbol{\Phi}_h(\mathbf{v}_h)\|_{\mathcal{Y}_h})$*.*

Then, from this result, the convergence of the numerical solution provided by (19)-(22) is directly obtained by means of the consistency and stability results (Theorem 2 and Theorem 3, respectively).

Theorem 5 *(Convergence of v) Assume the regularity hypotheses (H1)-(H4) on the data functions and the solution* $v(a,t)$*, and the disposal of approximations to the intrinsic survival probability* π_0 *that satisfy (H0). Considering that the numerical initial condition* $\mathbf{V}^0$ *is chosen such that, as* $h \to 0$

$$\|\mathbf{V}^0 - \mathbf{v}^0\|_{\infty,J+1} = o(h), \tag{61}$$

then, for h sufficiently small, there exists a unique solution $\mathbf{V}_h \in \mathcal{B}_{\mathcal{X}_h}(\mathbf{v}_h, R\,h)$ *of equations (19)-(22) and, as* $h \to 0$*,*

$$\|\mathbf{V}_h - \mathbf{v}_h\|_{\mathcal{X}_h} = \mathcal{O}(\|\mathbf{V}^0 - \mathbf{v}^0\|_{\infty,J+1} + h^2). \tag{62}$$

Remark 1 In particular, if $\mathbf{V}^0$ is the grid restriction $\mathbf{v}^0$ of the initial condition (14), then the scheme (19)-(22) is second order accurate for approximating v.

Now, we present the convergence theorem of the approximations given by (19)-(24) to the solution $u(a,t)$ to problem (1)-(3).

Theorem 6 *(Convergence of u) Assume the regularity hypotheses (H1)-(H4) on the data functions and the solutions* $u(a,t)$ *and* $v(a,t)$*, and the disposal of approximations* $\boldsymbol{\Pi}$ *to the intrinsic survival probability* π_0 *that satisfy (H0). Considering that the initial condition* u^0 *and its numerical approximation* $\mathbf{U}^0$ *are chosen such that, as* $h \to 0$

$$\left\| \frac{h\,\mathbf{u}^0}{\boldsymbol{\Pi}\cdot\boldsymbol{\pi}_0} \right\|_{\infty,J+1} = o(1), \qquad \left\| \frac{\mathbf{U}^0 - \mathbf{u}^0}{\boldsymbol{\Pi}} \right\|_{\infty,J+1} = o(h), \tag{63}$$

then, for h sufficiently small, there exists a unique solution $\mathbf{U}_h \in \mathcal{X}_h$ *of equations (19)-(24) and, as* $h \to 0$*,*

$$\|\mathbf{U}_h - \mathbf{u}_h\|_{\mathcal{X}_h} = \mathcal{O}\left(\left\| \frac{\mathbf{U}^0}{\boldsymbol{\Pi}} - \frac{\mathbf{u}^0}{\boldsymbol{\pi}_0} \right\|_{\infty,J+1} + h^2 \right), \tag{64}$$

where the product and the quotient of vectors must be considered in a componentwise sense.

Proof Quotients in (63) are well defined due to (H0) and the fact that the only point in which the intrinsic survival probability vanishes, the maximum age $a_\dagger$, is not a grid node.

Now, we check (61). From the definition of the initial conditions (23) and (14), we obtain the following bound for $j = 0, 1, \ldots, J$,

$$|V_j^0 - v_j^0| = \left| \frac{U_j^0}{\Pi_j} - \frac{u^0(a_j)}{\pi_0(a_j)} \right| \le \left| \frac{U_j^0 - u^0(a_j)}{\Pi_j} \right| + \left| \frac{u^0(a_j)}{\Pi_j\,\pi_0(a_j)} \right| |\Pi_j - \pi_0(a_j)|.$$

Thus, from hypothesis (H0) and (63), we conclude that, as $h \to 0$,

$$\|\mathbf{V}^0 - \mathbf{v}^0\|_{\infty, J+1} = o(h).$$

Then, on the one hand, Theorem 5 ensures the existence of a unique solution $\mathbf{V}_h \in \mathcal{B}_{\mathcal{X}_h}(\mathbf{v}_h, R\,h)$ of equations (19)-(22) and the behaviour of the error described in (62).

On the other hand, equations (24) and (11) allow us to arrive, for $n = 1, 2, \ldots, N$, $j = 0, 1, \ldots, J$, at

$$|U_j^n - u_j^n| = |\Pi_j\, V_j^n - \pi_0(a_j)\, v_j^n| \le |\Pi_j|\, |V_j^n - v_j^n| + |v_j^n|\, |\Pi_j - \pi_0(a_j)|, \tag{65}$$

which we combine with (62) and hypothesis (H0) to conclude (64). □

Remark 2 The same analysis gives second order of convergence if we further demand conditions on the initial data stronger than (63): for example, assuming that, as $h \to 0$,

$$\left\| \frac{\mathbf{u}^0}{\boldsymbol{\Pi} \cdot \boldsymbol{\pi}_0} \right\|_{\infty, J+1} = \mathcal{O}(1), \qquad \left\| \frac{\mathbf{U}^0 - \mathbf{u}^0}{\boldsymbol{\Pi}} \right\|_{\infty, J+1} = \mathcal{O}(h^2). \tag{66}$$

We would like to note that the first condition in (66) (and then, in (63)) imposes a specific decay of the initial data of the problem near the maximum age, and it depends not only on the size of the intrinsic survival probability (as in (16)), but also on the size of its approximation. This restriction is easily to satisfy if we consider an initial condition u^0 with compact support inside $[0, a_\dagger)$.

On the other hand, the second condition in (66) (and in (63)) establishes the degree of accuracy of the numerical initial data to the theoretical one, with respect to the size of the approximation to the intrinsic survival probability. This restriction is trivially achieved if, for example, we start the numerical method with the grid restriction of the theoretical initial data u^0.

4 Numerical results

In this section we corroborate the convergence results, previously demonstrated, through representative numerical simulations. To this end, we consider different test problems involving some of the vital parameters that have already been introduced in [15]. First of all, it is assumed that the vital functions depend on the density through the total size of the population

$$p(t) = \int_0^{a_\dagger} u(a, t)\, da, \qquad t \ge 0,$$

that is, the weight functions in (6) and (9), are $\gamma_\mu(a) = \gamma_\beta(a) = 1$.

For simplicity, a constant fertility rate is chosen $\beta(a, p, t) = \beta$, and the bounded component of the age-dependent mortality rate in (4) is considered to depend solely on population size $\mu_b(a, p, t) = \mu_b(p)$. In such a case, it is known that the exact solution to (1)-(3) has the separable expression

$$u(a, t) = \beta\, p(t)\, \pi_0(a)\, e^{-\sigma\, a}, \quad 0 \le a < a_\dagger,\; t \ge 0, \tag{67}$$

where π_0 is the intrinsic survival probability (7), depending on the unbounded mortality rate μ_0 considered in (4). On the other hand, the value of the parameter σ in (67) satisfies the nonlinear equation

$$\beta \int_0^{a_\dagger} \pi_0(a)\, e^{-\sigma\, a}\, da = 1. \tag{68}$$

Therefore, in order to obtain the expression of the solution to the model, chosen a maximum age $a_\dagger$, a natural mortality rate μ_0 (and then, the corresponding intrinsic survival probability π_0), and a value of the constant fertility rate β, then the corresponding value of the parameter σ is computed by solving (68). Note that if

$$\beta \int_0^{a_\dagger} \pi_0(a)\, da > 1,$$

then there exists a unique $\sigma > 0$ that satisfies (68).

In the numerical experiments, the bounded mortality rate is contemplated as in [15]: $\mu_b(p) = p$. In such a case, the total population is

$$p(t) = \frac{\sigma\, p_0}{p_0 + (\sigma - p_0)\, e^{-\sigma\, t}}, \qquad t \geq 0, \tag{69}$$

where p_0 represents the initial total population. Therefore, a preset value of the total population p_0, provides the total size population at each time level from (69) to arrive, finally, to $u(a, t)$ in (67), the exact solution to (1)-(3) with initial value

$$u^0(a) = \beta\, p_0\, \pi_0(a)\, e^{-\sigma\, a}, \quad 0 \leq a < a_\dagger. \tag{70}$$

In order to check the validity of the convergence Theorem 6, it is necessary to assume that the hypotheses about the initial data are fulfilled. But, it is not clear how the initial condition (70) satisfies the first hypothesis in (63). However, for $\sigma > 0$, if we consider a sufficiently large maximum age, the function $u^0(a)/\pi_0(a)$, and its derivatives up to a certain order, take very small values just before $a_\dagger$. Therefore, if we truncate u^0, nullifying it near the maximum age (that is, we construct a function with compact support strictly contained inside $[0, a_\dagger)$), then we obtain an initial condition that trivially verifies such hypothesis and, moreover, it can be accepted as a sufficiently smooth function, at least numerically up to a certain degree of precision in its computational representation. Even more, the choice of the grid restriction of this compact support function, as initial data of the numerical method, would avoid the possible difficulties that the calculation of the quotient (23) entails. With this in mind, for the numerical experiments to be presented here we have found that it is appropriate to assume $a_\dagger = 10$.

With respect to the natural mortality rate, and the relevance of using adequate approximations to it fulfilling (H0), the following representative case, that is paradigmatic in the numerical solution of finite life-span age-structured population models (see [13, 15], for example), has been chosen:

$$\mu_0(a) = \frac{\lambda}{(a_\dagger - a)^\alpha}, \quad 0 \leq a < a_\dagger, \tag{71}$$

with $\lambda > 0$ and $\alpha \geq 1$. For this function, the explicit expression of the intrinsic survival probability is easily obtained

$$\pi_0(a) = \begin{cases} \exp\left\{ -\dfrac{\lambda}{\alpha - 1} \left(\dfrac{1}{(a_\dagger - a)^{\alpha-1}} - \dfrac{1}{a_\dagger^{\alpha-1}} \right) \right\}, & \text{if } \alpha > 1, \\ \left(1 - \dfrac{a}{a_\dagger}\right)^\lambda, & \text{if } \alpha = 1, \end{cases} \quad 0 \leq a < a_\dagger. \tag{72}$$

Finally, in the experiments, we set the constant fertility rate $\beta = 4$ and the initial population $p_0 = 1$.

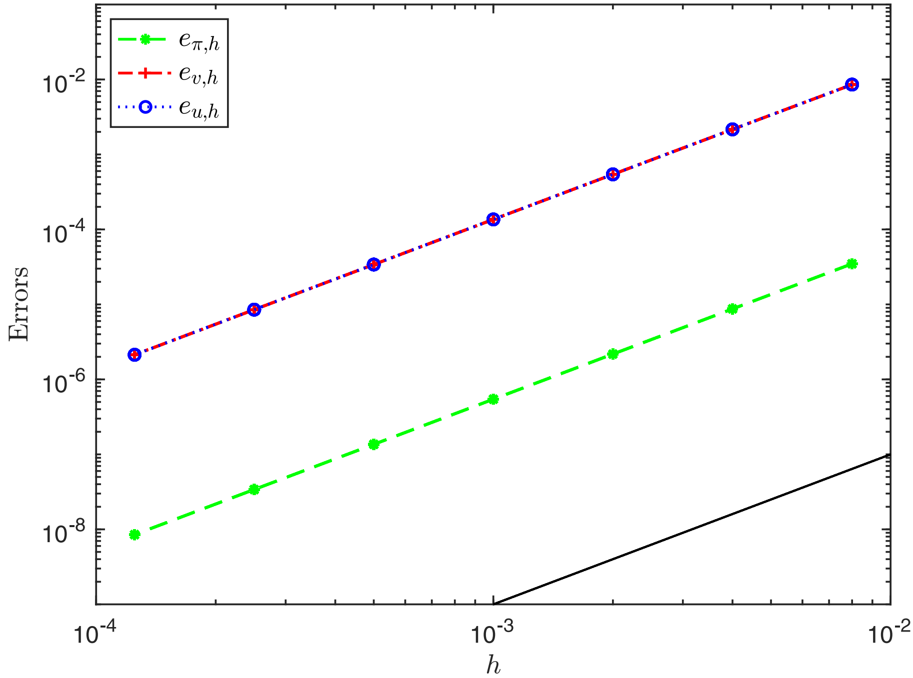

Fig. 1 Numerical errors involved in the simulation along the time interval [0, 1], for the natural mortality rate $\mu_0(a) = \dfrac{1}{(a_\dagger - a)^3}$. Line plotted in the lower right-hand corner represents slope 2

We have carried out simulations with the numerical scheme introduced in Section 2 over the time interval [0, 1]. Since the exact solution is known, we are able to show quantitatively the efficiency of the method.

Note that the natural mortality rate (71) does not incorporate an age a_* specifying a particular behaviour near the maximum age, therefore, given a positive integer J, we define the step size as $h = a_\dagger/(J+1)$.

In order to achieve approximations to the intrinsic survival probability π_0, associated to the mortality function (71), of which we know exactly how accurate they are, we consider the numerical method introduced in [1], that approximates the integral in (7) by means of the composite trapezoidal quadrature rule over an age grid.

For a value $h > 0$ of the step size, we denote the size of the global error in the approximation to the intrinsic survival probability as $e_{\pi,h} = \|\boldsymbol{\Pi} - \boldsymbol{\pi}_0\|_{\infty,J+1}$ (remember that vector $\boldsymbol{\pi}_0$ collects the exact values of the intrinsic survival probability over the age grid, and $\boldsymbol{\Pi}$ their numerical approximations); the size of the global error in the approximation to the density function as $e_{u,h} = \max_{n=0,\dots,N} \|\mathbf{U}^n - \mathbf{u}^n\|_{\infty,J+1}$ (now, at each time level n, $n = 0, 1, \dots N$, $\mathbf{u}^n$ contains the grid values of the exact solution (67) with σ satisfying (68) and p defined by (69), and $\mathbf{U}^n$ the numerical counterparts computed with the previously discussed numerical procedure (19)-(24)); and the size of the global error of the solution after the change of variable as $e_{v,h} = \max_{n=0,\dots,N} \|\mathbf{V}^n - \mathbf{v}^n\|_{\infty,J+1}$.

We start the experimentation with the natural mortality rate (71) for $\alpha > 1$. In this case, it is known that the numerical approximations to the survival probability offered by the numerical method in [1] are of second order for $\lambda > 0$. Here we present the results obtained

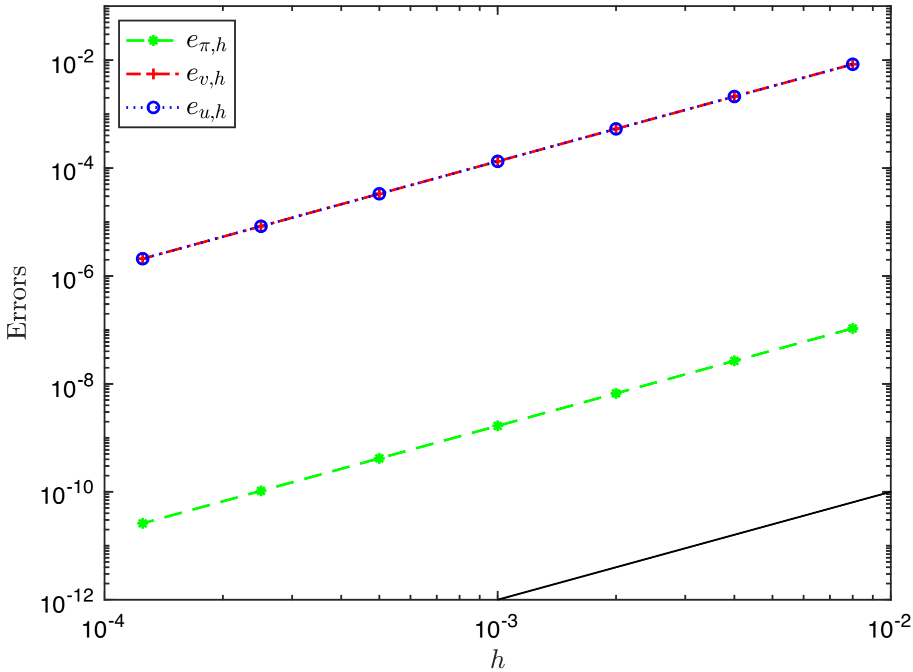

Fig. 2 Numerical errors involved in the simulation along the time interval [0, 1], for the natural mortality rate $\mu_0(a) = \dfrac{2}{a_\dagger - a}$. Line plotted in the lower right-hand corner represents slope 2

with $\lambda = 1$ and $\alpha = 3$: the numerical solution of the nonlinear equation (68) provides the value $\sigma = 3.99891639334478$.

Figure 1 shows, in logarithmic scale, the different errors involved in the simulation for the values of the step size $h = 10/1250$, $10/2500$, $10/5000$, $10/10000$, $10/20000$, $10/40000$, $10/80000$ (in the rest of the efficiency comparisons, the same values of the step size h are always considered). Dashed line corresponds to the errors $e_{\pi,h}$, dash-dotted line to the errors $e_{v,h}$, and dotted line to $e_{u,h}$ (this same way of representing the errors is used in the following graphs). Notice that these last two errors coincide in the simulation, and that this figure shows the expected second order of convergence in the all the different processes (as it is confirmed by the solid line plotted in the lower right-hand corner which represents the quadratic behaviour).

The next case corresponds to the natural mortality function (71) for $\alpha = 1$. Now, it is known that the numerical method in [1] provides approximations of second order when $\lambda \geq 2$. However, the order of convergence does deteriorate when $0 < \lambda < 2$: in such a case, simulations show that the effective order of convergence is only λ. Just these same conclusions are obtained for the numerical technique proposed in [13] for this mortality rate. Then, numerical experiments would address the role of precision in estimating the values of (72) on the general process of approximating the population density function, by taken different values of λ.

Firstly, we take $\lambda = 2$ for which second-order approximations to the survival probability are guaranteed. Now, according to (68), the value of the parameter in the exact solution is $\sigma = 3.79473725889754$. The results are in Figure 2, and the conclusion is just the same as in

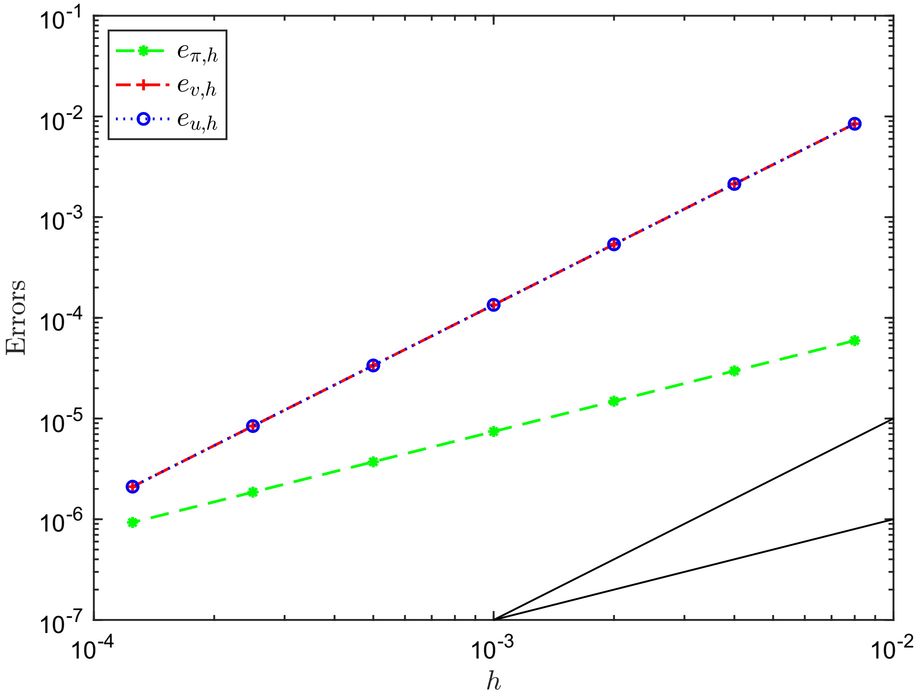

Fig. 3 Numerical errors involved in the simulation along the time interval [0, 1], for the natural mortality rate $\mu_0(a) = \dfrac{1}{a_\dagger - a}$. Lines plotted in the lower right-hand corner represents, from top to bottom, slopes 2 and 1, respectively

the previous experiment: second order in all the numerical approximations, and coincidence of the error in the approach of the density solutions, before and after the change of variable.

Now we will address the question of how the loss of accuracy in the estimation of the survival probability can affect the overall approximation process. For example, this case can be represented by $\lambda = 1$, where now $\sigma = 3.89736659610103$. The results are depicted in Figure 3. It is known that the numerical approximation to (72), offered by [1], is only first order as h decreases: this is corroborated by the linear slope that shows this error (dashed line). On the other hand, the approximation to the solution of the modified problem after the change of variable is, nonetheless, second order (dash-dotted line), which seems consistent with the thesis of Theorem 5 (convergence of v), due to the choice of the truncated initial data. However, despite the poor approximation in π_0, the error in the density function of the original problem is, still, second order (dotted line). Note that, this behaviour observed does not agree with that presented for the linear case in [2], although for a different test problem: there, $e_{\pi,h}$ and $e_{u,h}$ showed only first order although $e_{v,h}$ exhibited second order.

Moreover, we have observed this same behaviour for other values of $0 < \lambda < 2$, that cause a deterioration in the order of approximation to the survival probability. However, it does not seem to affect the effective order of the general approximation process to the density function. For example, similar observations can be made when $\lambda = 0.5$ (now $\sigma = 3.94868278711609$): Figure 4 shows that the order of convergence in the approximation of π_0 is 0.5, but the order of convergence in the approximation of u (and v) is still 2.

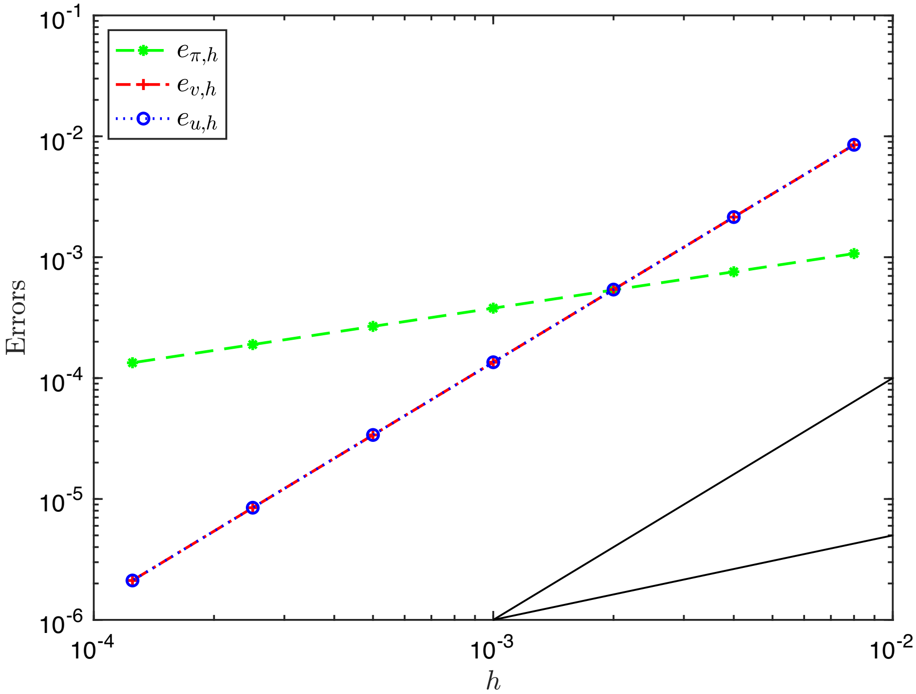

Fig. 4 Numerical errors involved in the simulation along the time interval [0, 1], for the natural mortality rate $\mu_0(a) = \dfrac{0.5}{a_\dagger - a}$. Lines plotted in the lower right-hand corner represents, from top to bottom, slopes 2 and 0.5, respectively

This discrepancy in the order of convergence shown in the global process with respect to the linear case, suggests that this situation is only justified by the nature of the simulation carried out here. So we have tried to understand this unexpected behaviour by Figure 5, that represents the different terms in inequality (65) for $\lambda = 0.5$, at the final time $T = 1$. The left column of pictures describes the age distribution of the errors, for the step sizes $h = 10/1250$ (dotted line) and $h = 10/12500$ (dash-dotted line): in the density solution u to the original problem (just, the left-hand side of (65)); in the solution v to the modified problem; and in the intrinsic part of the survival probability π_0 (these last two on the right-hand side of (65)), respectively. The right column of pictures presents: the age-distribution of the computed approximation to the survival probability $\boldsymbol{\Pi}$; and function v (again, both two on the right-hand side of (65)), respectively.

First of all, note that the age distributions of the error in u and in v are quite similar (first and second pictures on the left): in both cases, the maximum error is reached in births, and the distance between the errors obtained with the two considered values of h, certifies the second order of these approximations. Therefore, on the one hand, the error in v multiplied by the bounded size of the approximation $\boldsymbol{\Pi}$ to the survival probability (second row of pictures in Figure 5) gives second order terms in the estimate of the error in u given by (65). In addition, note that for newborns, the value of computed survival probability is equal to 1.

On the other hand, the last term on the right-hand size of (65), represents the age-distribution of the error in the approximation to π_0, multiplied by the bounded size of the

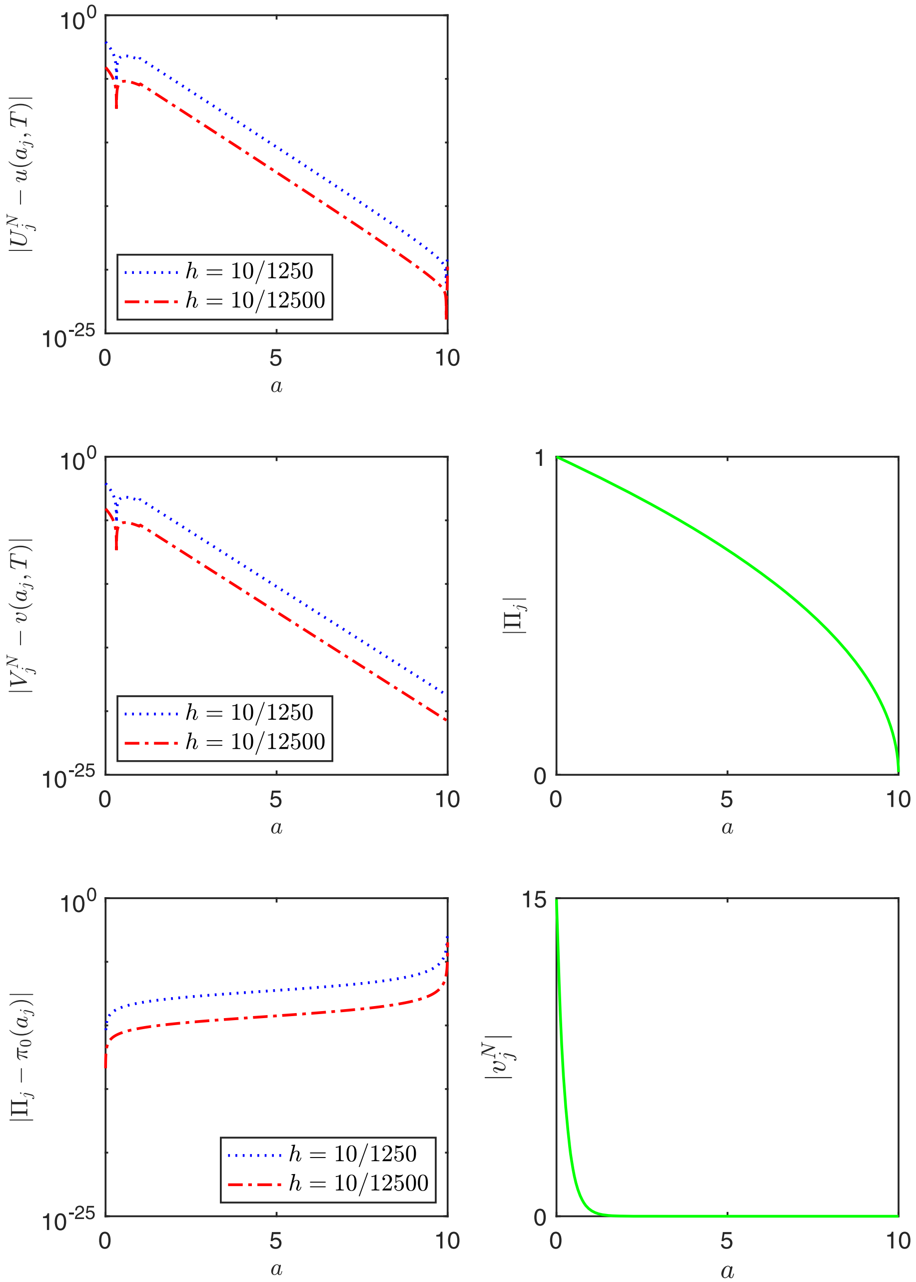

Fig. 5 Results obtained in the simulation at the final time $T = 1$, for the natural mortality rate $\mu_0(a) = \dfrac{0.5}{a_\dagger - a}$. Left: age distribution of the errors in u, v and π_0, respectively. Right: age distribution of the approximation $\boldsymbol{\Pi}$ and the exact function v, respectively

solution v. The convergence order in the approximation of the survival probability is known to deteriorate near the maximum age, which is where its maximum value is reached but, at the end of the age interval, the solution to the problem obtained after the change of variable is practically zero (see the third row of pictures in Figure 5). As a consequence, the product vanishes near $a_\dagger$, where the orden could be affected, keeping the second order of convergence certified at the beginning of the interval.

5 Conclusions

Mathematical models that describe population dynamics usually employ physiological age to structure the individuals in the population. In this context, age-structured population models with a finite life-span present a strong biological meaning. In addition, nonlinear models increase this significance because they consider the influence of the environment on the population through the dependence of the vital rates on functionals of the population density. However, the more realistic a model is, the more difficult it is to study. Thus, an analytical expression of the solution is not attainable in general nonlinear age-structured population problems, and the use of numerical techniques is an affordable manner to address the solution to these models.

In this paper, we have introduced a new procedure for the numerical approximation to the solution to (1)-(3). Convergence proofs of such approaches should circumvent the difficulties caused by the singularity of the mortality rate near the finite maximum age. By separating the numerical approximation of the intrinsic survival probability from the approximation to the age-dependent density, we can establish convergence of the numerical solution without an explicit dependence on the asymptotic growth behaviour of the natural mortality rate as in previous works. For this purpose, we reformulate the model problem (1)-(3) in terms of the age-dependent density function for the population rescaled with the intrinsic survival probability. This new variable is solution of an age-structured population model in which the effects of the singular natural mortality rate are limited through its influence on the intrinsic survival probability. By full discretization of this new problem (12)-(14), using given appropriate approximations to the intrinsic survival probability, we get a completely explicit scheme that arrives at the numerical solution to (1)-(3), after a preprocessing to obtain the new initial condition on the age grid and a postprocessing of the results achieved in the time evolution. Furthermore, we should point out that the numerical scheme is ready to use with given approximations to the intrinsic survival probability instead to a known expression of the natural mortality rate function.

This new numerical method has been completely analyzed under convenient regularity hypotheses on the data functions involved. For this purpose, we have studied its consistency and nonlinear stability properties to address its convergence in the following way. First, we have studied the convergence of the time evolution approximation of the solution to (12)-(14) (to this end, we have employed the discretization framework given in [18]) and next, we have extended this convergence result to the approach given to the solution to (1)-(3).

We have also provided a complete and representative numerical experimentation that corroborates the convergence results. We have observed that, even though the order of the approximation to the survival probability deteriorates, we recover the second-order of convergence to the age-dependent density function for the population $u(a, t)$, due to the fact that the approximations to the age-dependent density function scaled with the survival probability, $v(a, t)$, are decreasing to zero when the age approaches to the maximum age.

Acknowledgements The authors were supported in part by project PID2020-113554GB-I00/AEI/10.13039/501100011033 of the Spanish Agencia Estatal de Investigación, and Grant RED2022-134784-T by MCIN/AEI/10.13039/501100011033.

Funding Open access funding provided by FEDER European Funds and the Junta de Castilla y León under the Research and Innovation Strategy for Smart Specialization (RIS3) of Castilla y León 2021-2027.

Declarations

Conflicts of Interest The authors declare that they have no conflict of interest.

References

1. Abia, L.M., Angulo, O., López-Marcos, J.C., López-Marcos, M.A.: Approximating the survival probability in finite life-span population models. J. Comput. Appl. Math. **330**, 783–793 (2018). https://doi.org/10.1016/j.cam.2017.05.004
2. Abia, L.M., Angulo, O., López-Marcos, J.C., López-Marcos, M.A.: Numerical approximation of finite life-span age-structured population models. Math. Methods Appl. Sci. **45**, 3272–3283 (2022). https://doi.org/10.1002/mma.7136
3. Angulo, O., López-Marcos, J.C., López-Marcos, M.A., Martínez-Rodríguez, J.: Numerical analysis of an open marine population model with spaced-limited recruitment. Math. Comput. Modell. **52**, 1037–1044 (2010). https://doi.org/10.1016/j.mcm.2010.02.020
4. Angulo, O., López-Marcos, J.C., López-Marcos, M.A., Martínez-Rodríguez, J.: Numerical investigation of the recruitment process in open marine population models. J. Stat. Mech: Theory Exp. **2011**, P01003 (2011). https://doi.org/10.1088/1742-5468/2011/01/P01003
5. Angulo, O., López-Marcos, J.C., López-Marcos, M.A., Martínez-Rodríguez, J.: Numerical analysis of a population model of marine invertebrates with different life stages. Commun. Nonlinear Sci. Numer. Simul. **18**, 2153–2163 (2013). https://doi.org/10.1016/j.cnsns.2013.01.009
6. Angulo, O., López-Marcos, J.C., López-Marcos, M.A., Martínez-Rodríguez, J.: An age-structured population model with delayed and space-limited recruitment. Commun. Nonlinear Sci. Numer. Simul. **112**, 106545 (2022). https://doi.org/10.1016/j.cnsns.2022.106545
7. Angulo, O., López-Marcos, J.C., López-Marcos, M.A., Milner, F.A.: A numerical method for nonlinear age-structured population models with finite maximum age. J. Math. Anal. Appl. **361**, 150–160 (2010). https://doi.org/10.1016/j.jmaa.2009.09.001
8. Angulo, O., López-Marcos, J.C., Milner, F.A.: The application of an age-structured model with unbounded mortality to demography. Math. Biosci. **208**, 495–520 (2008). https://doi.org/10.1016/j.mbs.2006.11.001
9. Coyle, C., Nigam, N.: High-order Discontinuous Galerkin Methods for a class of transport equations with structured populations. Comput. Math. Appl. **72**, 768–784 (2016). https://doi.org/10.1016/j.camwa.2016.05.024
10. Cusulin, C., Gerardo-Giorda, L.: A numerical method for spatial diffusion in age-structured populations. Numer. Methods Partial Differ. Equations **26**, 253–273 (2010). https://doi.org/10.1002/num.20425
11. Iannelli, M.: Mathematical Theory of Age-Structured Population Dynamics. C.N.R., Giardini Editori e Stampatori, Pisa, Applied Mathematics Monographs (1995)
12. Iannelli, M., Milner, F.A.: The Basic Approach to Age-Structured Population Dynamics. Springer, Dordrecht, The Netherlands (2017)
13. Iannelli, M., Milner, F.A.: On the approximation of the Lotka-McKendrick equation with finite life-span. J. Comput. Appl. Math. **136**, 245–254 (2001). https://doi.org/10.1016/S0377-0427(00)00616-6

14. Kim, M.Y.: Discontinuous-Continuous Galerkin Methods for a Structured Model of a Biological System. SIAM J. Sci. Comput. **31**, 913–938 (2008). https://doi.org/10.1137/070706094
15. Kim, M.Y., Kwon, Y.: A collocation method for the Gurtin-MacCamy equation with finite life-span. SIAM J. Numer. Anal. **39**, 1914–1937 (2002). https://doi.org/10.1137/S0036142900370927
16. Kim, M.Y., Selenge, T.: Age-time continuous galerkin methods for a model of population dynamics. J. Comput. Appl. Math. **223**, 659–671 (2009). https://doi.org/10.1016/j.cam.2008.02.004
17. Kim, M.Y., Selenge, T.: Discontinuous-continuous galerkin methods for population diffusion with finite life span. Math. Popul. Stud. **23**, 17–36 (2016). https://doi.org/10.1080/08898480.2013.836428
18. López-Marcos, J.C., Sanz-Serna, J.M.: Stability and convergence in numerical analysis III: Linear investigation of nonlinear stability. IMA J. Numer. Anal. **8**, 71–84 (1988). https://doi.org/10.1093/imanum/8.1.71
19. Pelovska G.: An improved explicit scheme for age-dependent population model with spatial diffusion. Int. J. Numer. Anal. Model., **5**, 466–490 (2008). https://doi.org/2008-IJNAM-822
20. Pelovska, G., Iannelli, M.: Numerical methods for the Lotka-McKendrick's equation. J. Comput. Appl. Math. **197**, 534–557 (2006). https://doi.org/10.1016/j.cam.2005.11.033